XIV

Optics of metals

So far we have been concerned with the propagation of light in nonconducting, isotropic media. We now turn our attention to the optics of conducting media, more particularly to metals. An ordinary piece of metal is a crystalline aggregate, consisting of small crystals of random orientation. Single crystals of appreciable size are rare, but can be produced artificially; their optical properties will be studied in Chapter XV. A mixture of randomly oriented crystallites behaves evidently as an isotropic substance, and as the theory of light propagation in a conducting isotropic medium is much simpler than in a crystal, we shall consider it here in some detail.

According to §1.1, conductivity is connected with the appearance of Joule heat. This is an irreversible phenomenon, in which the electromagnetic energy is destroyed, or more precisely transformed into heat, and in consequence an electromagnetic wave in a conductor is attenuated. In metals, on account of their very high conductivity, this effect is so large that they are practically opaque. In spite of this, metals play an important part in optics. Strong absorption is accompanied by high reflectivity, so that metallic surfaces act as excellent mirrors. Because of the partial penetration of light into a metal, it is possible to obtain information about the absorption constants and the mechanism of absorption from observations of the reflected light, even though the depth of penetration is small.

We shall first consider the purely formal results arising from the existence of conductivity, and then briefly discuss a simple, somewhat idealized, physical model for this process, based on the classical theory of the electron. This model accounts only roughly for some of the observed effects; a more precise model can only be obtained with the help of quantum mechanics and is thus outside the scope of this book. The formal theory will be illustrated by applications to two problems of practical interest: the optics of stratified media containing an absorbing element, and the diffraction of light by a metallic sphere.

A particularly attractive mathematical feature of the theory is that the existence of conductivity may be taken into account simply by introducing a complex dielectric constant (or complex index of refraction), instead of a real one. In metals the imaginary part is preponderant.

14.1 Wave propagation in a conductor

Consider a homogeneous isotropic medium of dielectric constant ε, permeability μ, and conductivity σ. Using the material equations §1.1 (9)–(11), viz. $\mathbf{j} = \sigma\mathbf{E}$, $\mathbf{D} = \varepsilon\mathbf{E}$,

https://doi.org/10.1017/9781108769914.017 Published online by Cambridge University Press

$\mathbf{B} = \mu\mathbf{H}$, Maxwell's equations take the form

$$\operatorname{curl}\mathbf{H} - \frac{\varepsilon}{c}\dot{\mathbf{E}} = \frac{4\pi}{c}\sigma\mathbf{E}, \tag{1}$$

$$\operatorname{curl}\mathbf{E} + \frac{\mu}{c}\dot{\mathbf{H}} = 0, \tag{2}$$

$$\operatorname{div}\mathbf{E} = \frac{4\pi}{\varepsilon}\rho, \tag{3}$$

$$\operatorname{div}\mathbf{H} = 0. \tag{4}$$

It is easy to see that for an electromagnetic disturbance, incident from outside onto the conductor, one may replace (3) by $\operatorname{div}\mathbf{E} = 0$. For if we take the divergence of (1) and use (3) we obtain

$$-\frac{\varepsilon}{c}\operatorname{div}\dot{\mathbf{E}} = \frac{4\pi\sigma}{c}\frac{4\pi}{\varepsilon}\rho.$$

Also, differentiation of (3) with respect to time gives

$$\operatorname{div}\dot{\mathbf{E}} = \frac{4\pi}{\varepsilon}\dot{\rho}.$$

Eliminating $\operatorname{div}\dot{\mathbf{E}}$ between the last two equations one obtains

$$\dot{\rho} + \frac{4\pi\sigma}{\varepsilon}\rho = 0, \tag{5}$$

giving on integration

$$\rho = \rho_0 \mathrm{e}^{-t/\tau}, \qquad \text{where } \tau = \frac{\varepsilon}{4\pi\sigma}. \tag{6}$$

Any electric charge density ρ is thus seen to fall off exponentially with time. The *relaxation time* τ is exceedingly small for any medium having appreciable conductivity. For metals, this time is very much shorter (typically of the order of 10^{-18} s) than the periodic time of vibration of the wave. We may, therefore, assume that ρ in a metal is always sensibly zero. Consequently (3) may be written as

$$\operatorname{div}\mathbf{E} = 0. \tag{7}$$

From (1) and (2) it follows by elimination of $\mathbf{H}$ and the use of (7) that $\mathbf{E}$ satisfies the wave equation

$$\nabla^2\mathbf{E} = \frac{\mu\varepsilon}{c^2}\ddot{\mathbf{E}} + \frac{4\pi\mu\sigma}{c^2}\dot{\mathbf{E}}. \tag{8}$$

The term in $\dot{\mathbf{E}}$ implies that the wave is damped, i.e. it suffers a progressive attenuation as it is propagated through the medium.

If the field is strictly monochromatic, and of angular frequency ω, i.e. if $\mathbf{E}$ and $\mathbf{H}$ are of the form $\mathbf{E} = \mathbf{E}_0\mathrm{e}^{-\mathrm{i}\omega t}$, $\mathbf{H} = \mathbf{H}_0\mathrm{e}^{-\mathrm{i}\omega t}$, we have $\partial/\partial t \equiv -\mathrm{i}\omega$ so that (1) and (2) may be re-written as

$$\operatorname{curl}\mathbf{H} + \frac{\mathrm{i}\omega}{c}\left(\varepsilon + \mathrm{i}\frac{4\pi\sigma}{\omega}\right)\mathbf{E} = 0, \tag{9}$$

https://doi.org/10.1017/9781108769914.017 Published online by Cambridge University Press

$$\operatorname{curl}\mathbf{E} - \frac{\mathrm{i}\omega\mu}{c}\mathbf{H} = 0, \tag{10}$$

and (8) becomes

$$\nabla^2\mathbf{E} + \hat{k}^2\mathbf{E} = 0, \tag{11}$$

where

$$\hat{k}^2 = \frac{\omega^2\mu}{c^2}\left(\varepsilon + \mathrm{i}\frac{4\pi\sigma}{\omega}\right). \tag{12}$$

These equations are formally identical with the corresponding equations for nonconducting media if in the latter the dielectric constant ε (which, to a good approximation, was shown to be real except for frequencies ω that are close to a resonance — see §2.3.4) is replaced by

$$\hat{\varepsilon} = \varepsilon + \mathrm{i}\frac{4\pi\sigma}{\omega}. \tag{13}$$

The analogy with nonconducting media becomes closer still if, in addition to the complex wave number $\hat{k}$ and the complex dielectric constant $\hat{\varepsilon}$, we also introduce a complex phase velocity $\hat{v}$ and a complex refractive index $\hat{n}$ which, in analogy with §1.2 (8), §1.2 (12), and §1.3 (21), are defined by

$$\hat{v} = \frac{c}{\sqrt{\mu\hat{\varepsilon}}}, \qquad \hat{n} = \frac{c}{\hat{v}} = \sqrt{\mu\hat{\varepsilon}} = \frac{c}{\omega}\hat{k}. \tag{14}$$

We set

$$\hat{n} = n(1 + \mathrm{i}\kappa), \tag{15}$$

where n and κ are real, and we call κ *the attenuation index*.* The quantities n and κ may easily be expressed in terms of the material constants ε, μ and σ. Squaring (15) we have

$$\hat{n}^2 = n^2(1 + 2\mathrm{i}\kappa - \kappa^2). \tag{15a}$$

Also, from (14) and (13),

$$\hat{n}^2 = \mu\hat{\varepsilon} = \mu\left(\varepsilon + \mathrm{i}\frac{4\pi\sigma}{\omega}\right). \tag{16}$$

Now σ, just like ε, is not a true constant of the medium, but depends on the frequency. We will see later (§14.3) that for sufficiently low frequencies (long wavelengths) σ is, to a good approximation, real. Assuming that ε is also real, we obtain in this case, upon equating the real and imaginary parts in (15a) and (16), the following relations:

$$n^2(1 - \kappa^2) = \mu\varepsilon, \tag{16a}$$

$$n^2\kappa = \frac{2\pi\mu\sigma}{\omega} = \frac{\mu\sigma}{\nu}. \tag{16b}$$

From these equations it follows that

* The term 'extinction coefficient' is also used.

https://doi.org/10.1017/9781108769914.017 Published online by Cambridge University Press

$$n^2 = \frac{1}{2}\left(\sqrt{\mu^2\varepsilon^2 + \frac{4\mu^2\sigma^2}{\nu^2}} + \mu\varepsilon\right), \tag{17a}$$

$$n^2\kappa^2 = \frac{1}{2}\left(\sqrt{\mu^2\varepsilon^2 + \frac{4\mu^2\sigma^2}{\nu^2}} - \mu\varepsilon\right). \tag{17b}$$

The positive sign of the square roots is taken here, since n and $n\kappa$ are real, and consequently n^2 and $n^2\kappa^2$ must be positive.

Eq. (11) is formally identical with the wave equation for a nonconducting medium, but the wave number is now complex. The simplest solution is that of a plane, time-harmonic wave

$$\mathbf{E} = \mathbf{E}_0\, \mathrm{e}^{\mathrm{i}[\hat{k}\mathbf{r}\cdot\mathbf{s} - \omega t]}. \tag{18}$$

If, in accordance with (14) and (15), we substitute for $\hat{k}$ from the relation $\hat{k} = \omega\hat{n}/c = \omega n(1 + \mathrm{i}\kappa)/c$, (18) becomes

$$\mathbf{E} = \mathbf{E}_0\, \mathrm{e}^{-\frac{\omega}{c}n\kappa\mathbf{r}\cdot\mathbf{s}}\, \mathrm{e}^{\mathrm{i}\omega[\frac{n}{c}\mathbf{r}\cdot\mathbf{s} - t]}.$$

The real part of this expression, viz.

$$\mathbf{E} = \mathbf{E}_0\, \mathrm{e}^{-\frac{\omega}{c}n\kappa\mathbf{r}\cdot\mathbf{s}} \cos\left\{\omega\left[\frac{n}{c}\mathbf{r}\cdot\mathbf{s} - t\right]\right\}, \tag{19}$$

which represents the electric vector, is a plane wave with wavelength $\lambda = 2\pi c/\omega n$ and with attenuation given by the exponential term. Since the energy density w of the wave is proportional to the time average of $\mathbf{E}^2$, it follows that w decreases in accordance with the relation

$$w = w_0\, \mathrm{e}^{-\chi\mathbf{r}\cdot\mathbf{s}}, \tag{20}$$

where

$$\chi = \frac{2\omega}{c}n\kappa = \frac{4\pi\nu}{c}n\kappa = \frac{4\pi}{\lambda_0}n\kappa = \frac{4\pi}{\lambda}\kappa, \tag{21}$$

λ_0 being the wavelength in vacuum and λ the wavelength in the medium. The constant χ [denoted by α in §4.11 (6)] is called *the absorption coefficient*.

The energy density falls to $1/\mathrm{e}$ of its value after the wave has advanced a distance d, where

$$d = \frac{1}{\chi} = \frac{\lambda_0}{4\pi n\kappa} = \frac{\lambda}{4\pi\kappa}. \tag{22}$$

This quantity is usually a very small fraction of the wavelength (see Table 14.1).*

Returning to (17) we see that, when $\sigma = 0$, the first equation correctly reduces to Maxwell's relation §1.2 (14) $n^2 = \mu\varepsilon$, and the second gives $\kappa = 0$. For metals $\sigma \neq 0$ and is in fact so large that in (17) ε may be neglected in comparison with $2\sigma/\nu$. To get an idea of the orders of magnitude involved let it be remarked that for most metals the conductivity at frequencies up to about the infra-red region of the spectrum

* This phenomenon of penetration to a depth that is a small fraction of the wavelength is well known in the conduction of alternating currents and is known to engineers as the 'skin effect.'

https://doi.org/10.1017/9781108769914.017 Published online by Cambridge University Press

Table 14.1. *The 'penetration depth' d for copper for radiation in three familiar regions of the spectrum, calculated with the static conductivity* $\sigma \sim 5.14 \times 10^{17}$ s^{-1} *and* $\mu = 1$.

Radiation	Infra-red	Microwaves	Long radio waves
λ_0	10^{-3} cm	10 cm	1000 m $= 10^5$ cm
d	6.1×10^{-7} cm	6.1×10^{-5} cm	6.1×10^{-3} cm

($\lambda \geqslant 10^{-3}$ cm) is of the order of 10^{17} s^{-1}. Thus, for example, with $\lambda = 10^{-3}$ cm ($\nu \sim 3 \times 10^{13}$ s^{-1}), one then has $\sigma/\nu \sim 3000$. The dielectric constant ε of a metal cannot be measured directly, but as we shall see it can be deduced from optical experiments. However, as the mechanism of electric polarization in metals is not fundamentally different from that of a dielectric, it may be assumed that ε is of the same order of magnitude. Hence, provided the wavelength is not too short, one may suppose that

$$\frac{\mu\sigma}{\nu} = n^2\kappa \gg \mu\varepsilon. \tag{23}$$

Eqs. (17) and (22) now reduce to

$$n \sim n\kappa = \sqrt{\frac{\mu\sigma}{\nu}}, \tag{24}$$

$$d \sim \frac{\lambda_0}{4\pi}\sqrt{\frac{\nu}{\mu\sigma}} = \frac{1}{4\pi}\sqrt{\frac{c\lambda_0}{\mu\sigma}} = \frac{c}{\sqrt{8\pi\mu\sigma\omega}}. \tag{25}$$

A perfect conductor is characterized by infinitely large conductivity ($\sigma \to \infty$). Since according to (16), $\varepsilon/\sigma = (1 - \kappa^2)/\nu\kappa$, we have in this limiting case $\kappa^2 \to 1$, or by (16a), $n \to \infty$. Such a conductor would not permit the penetration of an electromagnetic wave to any depth at all and would reflect all the incident light (see §14.2 below).

Whilst the refractive index of transparent substances may easily be measured from the angle of refraction, such measurements are extremely difficult to carry out for metals, because a specimen of the metal which transmits any appreciable fraction of incident light has to be exceedingly thin. Nevertheless Kundt* succeeded in constructing metal prisms that enabled direct measurements of the real and imaginary parts of the complex refractive index to be made. Usually, however, the optical constants of metals are determined by means of katoptric rather than dioptric experiments, i.e. by studying the changes which light undergoes on reflection from a metal, rather than by means of measurements on the light transmitted through it.

14.2 Refraction and reflection at a metal surface

We have seen that the basic equations relating to the propagation of a plane time-harmonic wave in a conducting medium differ from those relating to propagation in a transparent dielectric only in that the real constants ε and k are replaced by complex

* A. Kundt, *Ann. d. Physik*, **34** (1888), 469.

https://doi.org/10.1017/9781108769914.017 Published online by Cambridge University Press

constants $\hat{\varepsilon}$ and $\hat{k}$. It follows that the formulae derived in Chapter I, as far as they involve only linear relations between the components of the field vectors of plane monochromatic waves, apply also in the present case. In particular, the boundary conditions for the propagation of a wave across a surface of discontinuity and hence also the formulae of §1.5 relating to refraction and reflection remain valid.

Consider first the propagation of a plane wave from a dielectric into a conductor, both media being assumed to be of infinite extent, the surface of contact between them being the plane $z = 0$. By analogy with §1.5 (8) the law of refraction is

$$\sin\theta_t = \frac{1}{\hat{n}}\sin\theta_i. \tag{1}$$

Since $\hat{n}$ is complex, so is θ_t, and this quantity therefore no longer has the simple significance of an angle of refraction.

Let the plane of incidence be the x, z-plane. The space-dependent part of the phase of the wave in the conductor is given by $\hat{k}\mathbf{r}\cdot\mathbf{s}^{(t)}$, where [see §1.5 (4)]

$$s_x^{(t)} = \sin\theta_t, \qquad s_y^{(t)} = 0, \qquad s_z^{(t)} = \cos\theta_t. \tag{2}$$

From (1) and (2) and §14.1 (15)

$$s_x^{(t)} = \sin\theta_t = \frac{\sin\theta_i}{n(1+\mathrm{i}\kappa)} = \frac{1-\mathrm{i}\kappa}{n(1+\kappa^2)}\sin\theta_i, \tag{3a}$$

$$\begin{aligned} s_z^{(t)} = \cos\theta_t &= \sqrt{1-\sin^2\theta_t} \\ &= \sqrt{1-\frac{(1-\kappa^2)}{n^2(1+\kappa^2)^2}\sin^2\theta_i + \mathrm{i}\frac{2\kappa}{n^2(1+\kappa^2)^2}\sin^2\theta_i}. \end{aligned} \tag{3b}$$

It is convenient to express $s_z^{(t)}$ in the form

$$s_z^{(t)} = \cos\theta_t = q\,\mathrm{e}^{\mathrm{i}\gamma} \tag{4}$$

(q, γ real). Expressions for q and γ in terms of n, κ and $\sin\theta_i$ are immediately obtained on squaring (3b) and (4) and equating real and imaginary parts. This gives

$$\left.\begin{aligned} q^2\cos 2\gamma &= 1 - \frac{1-\kappa^2}{n^2(1+\kappa^2)^2}\sin^2\theta_i, \\ q^2\sin 2\gamma &= \frac{2\kappa}{n^2(1+\kappa^2)^2}\sin^2\theta_i. \end{aligned}\right\} \tag{5}$$

It follows that

$$\begin{aligned} \hat{k}\mathbf{r}\cdot\mathbf{s}^{(t)} &= \frac{\omega}{c}n(1+\mathrm{i}\kappa)(xs_x^{(t)} + zs_z^{(t)}) \\ &= \frac{\omega}{c}n(1+\mathrm{i}\kappa)\left[\frac{x(1-\mathrm{i}\kappa)}{n(1+\kappa^2)}\sin\theta_i + z(q\cos\gamma + iq\sin\gamma)\right] \\ &= \frac{\omega}{c}[x\sin\theta_i + znq(\cos\gamma - \kappa\sin\gamma) + \mathrm{i}nzq(\kappa\cos\gamma + \sin\gamma)]. \end{aligned} \tag{6}$$

We see that the surfaces of constant amplitude are given by

$$z = \text{constant}, \tag{7}$$

https://doi.org/10.1017/9781108769914.017 Published online by Cambridge University Press

and are, therefore, planes parallel to the boundary. The surfaces of constant real phase are given by

$$x \sin\theta_i + znq(\cos\gamma - \kappa\sin\gamma) = \text{constant}, \tag{8}$$

and are planes whose normals make an angle θ_t' with the normal to the boundary, where

$$\left.\begin{aligned} \cos\theta_t' &= \frac{nq(\cos\gamma - \kappa\sin\gamma)}{\sqrt{\sin^2\theta_i + n^2q^2(\cos\gamma - \kappa\sin\gamma)^2}}, \\ \sin\theta_t' &= \frac{\sin\theta_i}{\sqrt{\sin^2\theta_i + n^2q^2(\cos\gamma - \kappa\sin\gamma)^2}}. \end{aligned}\right\} \tag{9}$$

Since the surfaces of constant amplitude and the surfaces of constant phase do not in general coincide with each other, the wave in the metal is an *inhomogeneous wave*.

If we denote the square root in (9) by n', the equation for $\sin\theta_t'$ may be written in the form $\sin\theta_t' = \sin\theta_i/n'$, i.e. it has the form of Snell's law. However, n' depends now not only on the quantities that specify the medium, but also on the angle of incidence θ_i.

We may also derive expressions for the amplitude and the phase of the refracted and reflected waves by substituting for θ_t the complex value given by (1) in the Fresnel formulae (§1.5.2). The explicit expressions will be given in §14.4.1 in connection with the theory of stratified conducting media. Here we shall consider how the optical constants of the metal may be deduced from observation of the reflected wave.

Since we assumed that the first medium is a dielectric, the reflected wave is an ordinary (homogeneous) wave with a real phase factor. As in §1.5 (21a) the amplitude components $A_\parallel$, $A_\perp$ of the incident wave and the corresponding components $R_\parallel$, $R_\perp$ of the reflected wave are related by

$$\left.\begin{aligned} R_\parallel &= \frac{\tan(\theta_i - \theta_t)}{\tan(\theta_i + \theta_t)} A_\parallel, \\ R_\perp &= -\frac{\sin(\theta_i - \theta_t)}{\sin(\theta_i + \theta_t)} A_\perp. \end{aligned}\right\} \tag{10}$$

Since θ_t is now complex, so are the ratios $R_\parallel/A_\parallel$ and $R_\perp/A_\perp$, i.e. characteristic phase changes occur on reflection; thus incident linearly polarized light will in general become elliptically polarized on reflection at the metal surface. Let $\phi_\parallel$ and $\phi_\perp$ be the phase changes, and $\rho_\parallel$ and $\rho_\perp$ the absolute values of the reflection coefficients, i.e.

$$r_\parallel = \frac{R_\parallel}{A_\parallel} = \rho_\parallel e^{i\phi_\parallel}, \qquad r_\perp = \frac{R_\perp}{A_\perp} = \rho_\perp e^{i\phi_\perp}. \tag{11}$$

Suppose that the incident light is *linearly polarized* in the azimuth α_i, i.e.

$$\tan\alpha_i = \frac{A_\perp}{A_\parallel}, \tag{12}$$

and let α_r be the azimuthal angle (generally complex) of the light that is reflected. Then*

* We write $-i\Delta$ rather than $+i\Delta$ in the exponent on the right-hand side of (13) to facilitate comparison with certain results of §1.5.

https://doi.org/10.1017/9781108769914.017 Published online by Cambridge University Press

$$\tan\alpha_r = \frac{R_\perp}{R_\parallel} = -\frac{\cos(\theta_i - \theta_t)}{\cos(\theta_i + \theta_t)} \tan\alpha_i = P\,\mathrm{e}^{-\mathrm{i}\Delta} \tan\alpha_i, \tag{13}$$

where

$$P = \frac{\rho_\perp}{\rho_\parallel}, \qquad \Delta = \phi_\parallel - \phi_\perp. \tag{14}$$

We note that α_r is real in the following two cases:

(1) For normal incidence ($\theta_i = 0$); then $P = 1$ and $\Delta = -\pi$, so that $\tan\alpha_r = -\tan\alpha_i$.
(2) For grazing incidence ($\theta_i = \pi/2$); then $P = 1$ and $\Delta = 0$, so that $\tan\alpha_r = \tan\alpha_i$.

It should be remembered that in the case of normal incidence the directions of the incident and reflected rays are opposed; thus the negative sign implies that the azimuth of the linearly polarized light is unchanged in its absolute direction in space. It is also unchanged in its absolute direction when the incidence is grazing.

Between the two extreme cases just considered, there exists an angle $\overline{\theta}_i$ called the *principal angle of incidence* which is such that $\Delta = -\pi/2$. At this angle of incidence, linearly polarized light is, in general, reflected as elliptically polarized light, but as may be seen from §1.4 (31b) (with $\delta = \pi/2$), the axes of the vibration ellipse are parallel and perpendicular to the plane of incidence. If, moreover, $P\tan\alpha_i = 1$, then according to (13) $\tan\alpha_r = -\mathrm{i}$, and the reflected light is *circularly* polarized.

Suppose that with linearly polarized incident light an additional phase difference Δ is introduced between $R_\parallel$ and $R_\perp$ by means of a suitable compensator (see §15.4.2). The total phase difference is then zero, and, according to (13) the reflected light is linearly polarized in an azimuth α'_r such that

$$\tan\alpha'_r = P\tan\alpha_i. \tag{15}$$

The angle α'_r is, for obvious reasons, called *the angle of restored polarization*, though it is usually defined only with incident light that is *linearly polarized* in the azimuth* $\alpha_i = 45°$. The values of α'_r and P relating to the principal angle of incidence $\theta_i = \overline{\theta}_i$ will be denoted by $\overline{\alpha}'_r$ and $\overline{P}$ respectively. If we imagine a rectangle to be circumscribed around the vibration ellipse of the (uncompensated) reflected light obtained from light that is incident at the principal angle, with its sides parallel and perpendicular to the plane of incidence, then the sides are in the ratio $\overline{P}\tan\alpha_i$ and the angle between a diagonal and the plane of incidence is $\overline{\alpha}'_r$ (see Fig. 14.1).

For the purpose of later calculations it is useful to introduce an angle ψ such that

$$\tan\psi = P; \tag{16}$$

the value of ψ corresponding to the principal angle of incidence will be denoted by $\overline{\psi}$.

Using (10) and (1) we can compute the quantities P ($= \tan\psi$) and Δ in terms of θ_i, if the constants n and κ of the metal are known. Fig. 14.2(a) shows their dependence on θ_i in a typical case. In Fig. 14.2(b) analogous curves relating to reflection from a transparent dielectric are displayed for comparison. The sudden discontinuity from $-\pi$ to 0 in the value of Δ which occurs when light is reflected from a transparent dielectric

* Then α'_r is equal to the angle ψ introduced in (16).

https://doi.org/10.1017/9781108769914.017 Published online by Cambridge University Press

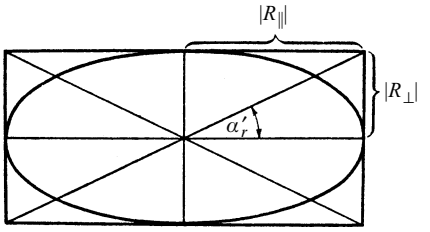

Fig. 14.1 Vibration ellipse of light reflected from a metal at the principal angle of incidence.

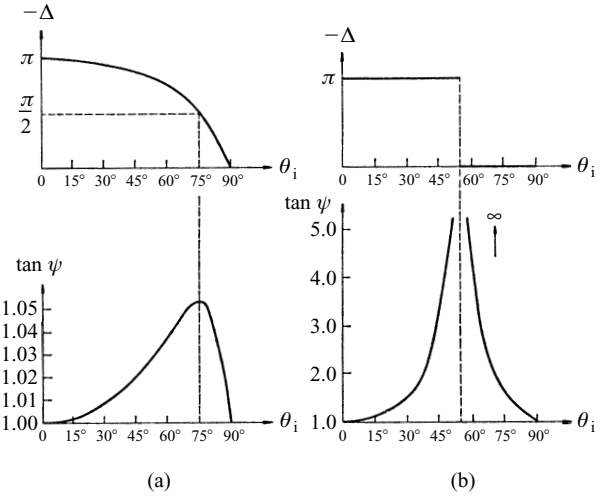

Fig. 14.2 The quantities $-\Delta = \phi_\perp - \phi_\parallel$ and $P = \tan\psi = \rho_\perp/\rho_\parallel$, which characterize the change in the state of polarization of light on reflection from a typical metal surface (a) and from a transparent dielectric (b).

at the polarizing angle is absent when light is reflected from a metal surface. The sharp cusp when $\tan\psi$ becomes infinite is likewise absent, and the curve is replaced by a smooth curve with a comparatively broad maximum. The angle of incidence at which this maximum occurs is sometimes called the *quasi-polarizing angle*; it is nearly equal to the principal angle of incidence $\overline{\theta}_i$. It is commonly assumed that this maximum is actually at $\overline{\theta}_i$, which is almost exactly true if $n^2(1+\kappa^2) \gg 1$, as is usually the case (cf. Table 7.3). In general the two angles are, however, different; for example, in the case of silver at the ultra-violet wavelength 3280 Å; the quantity $n^2(1+\kappa^2)$ is small; then $\overline{\theta}_i = 47.8°$ and $\psi = 31.8°$, whereas $\psi_{\max} = 29.5°$ and occurs at $\theta_i = 40°$, approximately.

Generally speaking the problem is not to find ψ and Δ from known values of n and κ, but to determine n and κ from experimental observations of the amplitude and phase of light reflected from the metal.

As the quantities $R_\parallel$, $R_\perp$, $\phi_\parallel$, $\phi_\perp$, ψ and Δ are all functions of θ_i, and of n and κ, measurement of any two of these quantities for a specific value of the angle of

https://doi.org/10.1017/9781108769914.017 Published online by Cambridge University Press

incidence θ_i will in general permit the evaluation of n and κ. Since in many experiments one determines the last two of these quantities, we shall derive the fundamental expressions for n and κ in terms of ψ and Δ. From (13) and (1)

$$\frac{1 - Pe^{-i\Delta}}{1 + Pe^{-i\Delta}} = -\frac{\cos\theta_i \cos\theta_t}{\sin\theta_i \sin\theta_t} = -\frac{\sqrt{\hat{n}^2 - \sin^2\theta_i}}{\sin\theta_i \tan\theta_i}. \tag{17}$$

Since $P = \tan\psi$, the left-hand side of (17) may be expressed in the form

$$\frac{1 - Pe^{-i\Delta}}{1 + Pe^{-i\Delta}} = \frac{1 - e^{-i\Delta}\tan\psi}{1 + e^{-i\Delta}\tan\psi} = \frac{\cos 2\psi + i \sin 2\psi \sin\Delta}{1 + \sin 2\psi \cos\Delta}. \tag{18}$$

From (17) and (18),

$$\frac{\sqrt{\hat{n}^2 - \sin^2\theta_i}}{\sin\theta_i \tan\theta_i} = -\frac{\cos 2\psi + i \sin 2\psi \sin\Delta}{1 + \sin 2\psi \cos\Delta}. \tag{19}$$

Now if, as is usually the case in the visible region,

$$n^2(1 + \kappa^2) \gg 1, \tag{20}$$

$\sin^2\theta_i$ may be neglected in comparison with $\hat{n}^2$ and we obtain

$$\frac{\hat{n}}{\sin\theta_i \tan\theta_i} = \frac{n(1 + i\kappa)}{\sin\theta_i \tan\theta_i} \sim -\frac{\cos 2\psi + i \sin 2\psi \sin\Delta}{1 + \sin 2\psi \cos\Delta}. \tag{21}$$

Equating the real parts, we obtain

$$n \sim -\frac{\sin\theta_i \tan\theta_i \cos 2\psi}{1 + \sin 2\psi \cos\Delta}. \tag{22a}$$

Equating the imaginary parts and using (22a) we find that

$$\kappa \sim \tan 2\psi \sin\Delta. \tag{22b}$$

These expressions permit the calculation of the optical constants n and κ from measurements of ψ and Δ at any angle of incidence. In the particular case of observation at the principal angle of incidence $\overline{\theta}_i$ one has $\Delta = -\pi/2$, $\psi = \overline{\psi}$ and (22a) and (22b) reduce to

$$n \sim -\sin\overline{\theta}_i \tan\overline{\theta}_i \cos 2\overline{\psi}, \tag{23a}$$

$$\kappa \sim -\tan 2\overline{\psi}. \tag{23b}$$

Other formulae relating to n and κ are sometimes useful. Without assuming (20) we have, on squaring (19),

$$\frac{\hat{n}^2 - \sin^2\theta_i}{\sin^2\theta_i \tan^2\theta_i} = \frac{\cos^2 2\psi - \sin^2 2\psi \sin^2\Delta + i \sin 4\psi \sin\Delta}{(1 + \sin 2\psi \cos\Delta)^2}. \tag{24}$$

If we substitute $\hat{n}^2 = n^2(1 - \kappa^2) + 2in^2\kappa$ and equate real and imaginary parts we obtain

https://doi.org/10.1017/9781108769914.017 Published online by Cambridge University Press

$$n^2(1-\kappa^2) = \sin^2\theta_i\left[1+\frac{\tan^2\theta_i(\cos^2 2\psi - \sin^2 2\psi \sin^2\Delta)}{(1+\sin 2\psi\cos\Delta)^2}\right], \tag{25a}$$

$$2n^2\kappa = \frac{\sin^2\theta_i \tan^2\theta_i \sin 4\psi \sin\Delta}{(1+\sin 2\psi\cos\Delta)^2}. \tag{25b}$$

In particular, at the principal angle of incidence ($\theta = \overline{\theta}_i$, $\Delta = -\pi/2$), these equations reduce to*

$$n^2(1-\kappa^2) = \sin^2\overline{\theta}_i(1+\tan^2\overline{\theta}_i\cos 4\overline{\psi}), \tag{26a}$$

$$2n^2\kappa = -\sin^2\overline{\theta}_i\tan^2\overline{\theta}_i\sin 4\overline{\psi}. \tag{26b}$$

The formulae (25) do not yield n and κ directly but in the combinations $n^2(1-\kappa^2)$ and $n^2\kappa$. On reference to §14.1 (16) we see that these quantities have a direct physical significance. With $\mu = 1$ (as is always the case at optical wavelengths), $n^2(1-\kappa^2)$ is the dielectric constant, and $n^2\kappa$ the ratio of the conductivity and the frequency. From the magnitude of these quantities, and particularly from their variation with frequency, information may be obtained about the structure of the metal (see §14.3 below).

So far our analysis has centred round the amplitudes of the components of the reflected light, but, as we shall see shortly, useful information may also be obtained from comparison of the intensity of the reflected light with that of the incident light, especially at long wavelengths. If we consider normal incidence ($\theta_i = 0$), the distinction between $R_\parallel$ and $R_\perp$ disappears, the plane of incidence then being undetermined, and we may write

$$\mathcal{R} = \left|\frac{R_\parallel}{A_\parallel}\right|^2 = \left|\frac{R_\perp}{A_\perp}\right|^2. \tag{27}$$

If we substitute from (1) and (10) (or if we replace n by $\hat{n}$ in §1.5 (23)), we obtain

$$\mathcal{R} = \left|\frac{\hat{n}-1}{\hat{n}+1}\right|^2 = \frac{n^2(1+\kappa^2)+1-2n}{n^2(1+\kappa^2)+1+2n}. \tag{28}$$

The optical constants of many metals have been determined from measurements of reflected light. In Table 14.2 values of the constants as found by various observers are given for a wavelength in the yellow region of the visible spectrum. The metals are arranged in order of their reflectivity $\mathcal{R}$. We note that in all cases $n < n\kappa$ so that according to §14.1 (16a) $\mu\varepsilon$ and consequently (since $\mu \sim 1$ at optical wavelengths) ε is negative. At first sight it might appear that no physical significance can be attached to a negative dielectric constant. We shall see later that this is not the case and that the negative value of ε can be explained from certain simple assumptions concerning the electron mechanism of conductivity. From the table it would appear that values† $n < 1$ are associated with high reflectivity but in general this is not the case.

* Equations such as (23) and (26), which involve measurements only at the principal angle of incidence, are simpler than the more general expressions (22) or (25), and for this reason alone many experimenters have restricted themselves to measurements at this angle. At other angles of incidence experimental accuracy may be greater. Convenient choice of the angle of incidence is discussed in P. Drude, *Ann. d. Physik*, **39** (1890), 504; J. R. Collins and R. O. Bock, *Rev. Sci. Instr.*, **14** (1943), 135; I. Simon, *J. Opt. Soc. Amer.*, **41** (1951), 336; D. G. Avery, *Proc. Phys. Soc.*, **65** (1952), 425; R. W. Ditchburn, *J. Opt. Soc. Amer.*, **45** (1955), 743.

† When $n < 1$, the real phase velocity c/n exceeds the velocity of light in vacuum, but as explained at the end of §1.3.3 this is not in contradiction with the theory of relativity.

https://doi.org/10.1017/9781108769914.017 Published online by Cambridge University Press

Table 14.2. *The optical constants of metals, for light of wavelength* $\lambda = 5893$ Å (*sodium D lines*).

Metal	n	$n\kappa$	$\mathcal{R}$	Observer	
Sodium, solid	0.044	2.42	0.97	Duncan	1913
Silver, massive	0.20	3.44	0.94	Oppitz	1917
Magnesium, massive	0.37	4.42	0.93	Drude	1890
Potassium, molten	0.084	1.81	0.92	Nathanson	1928
Cadmium, massive	1.13	5.01	0.84	Drude	1890
Aluminium, massive	1.44	5.23	0.83	Drude	1890
Tin, massive	1.48	5.25	0.83	Drude	1890
Gold, electrolytic	0.47	2.83	0.82	Meier	1910
Mercury, liquid	1.60	4.80	0.77	Lowery and Moore	1932
Zinc, massive	1.93	4.66	0.75	Meier	1910
Copper, massive	0.62	2.57	0.73	Oppitz	1917
Gallium, single crystal	3.69	5.43	0.71	Lange	1935
Antimony, massive	3.04	4.94	0.70	Drude	1890
Cobalt, massive	2.12	4.04	0.68	Minor	1904
Nickel, electrolytic	1.58	3.42	0.66	Meier	1910
Manganese, massive	2.41	3.88	0.64	Littleton	1911
Lead, massive	2.01	3.48	0.62	Drude	1890
Platinum, electrolytic	2.63	3.54	0.59	Meier	1910
Rhenium, massive	3.00	3.44	0.57	Lange	1935
Tungsten, massive	3.46	3.25	0.54	Littleton	1912
Bismuth, massive	1.78	2.80	0.54	Meier	1910
Iron, evaporated	1.51	1.63	0.33	Meier	1910

Condensed from H. H. Landolt and R. Börnstein, *Phys. Chem. Tabellen*, (5 Aufl., Berlin, 1923; 1–3 Ergänzungsb, Berlin, 1927–1936).

The values of n and $n\kappa$ displayed in Table 14.2 cannot be expected to be in agreement with calculations based on the approximate formulae §14.1 (17). These formulae were derived on the assumption that the conductivity σ is real and as we will see in §14.3 this assumption is fulfilled to a good approximation only at low frequencies. It will become clear from the considerations of §14.3 where we examine the frequency dependence of σ from an elementary model, that at the high frequencies ($\omega \sim 3.2 \times 10^{15}$ s^{-1}) corresponding to the sodium D lines, to which Table 14.2 refers, σ is complex, and its imaginary part is, in fact, appreciably larger than its real part. Indeed the dependence of the optical constants of metals on the wavelength, determined from experiments, shows a much more complicated behaviour than our formulae predict (see Fig. 14.3).

It appears from investigations of Hagen and Rubens* and subsequent workers that the reflectivity of many metals, calculated from the elementary theory that we outlined and with σ approximated by its static value, is in good agreement with results of experiments, provided the wavelength of the radiation λ is not shorter than about 10^{-3} cm. If we substitute for n and $n\kappa$ from §14.1 (24), (28) becomes (taking $\mu = 1$),

* E. Hagen and H. Rubens, *Ann. d. Physik* (4), **11** (1903), 873.

https://doi.org/10.1017/9781108769914.017 Published online by Cambridge University Press

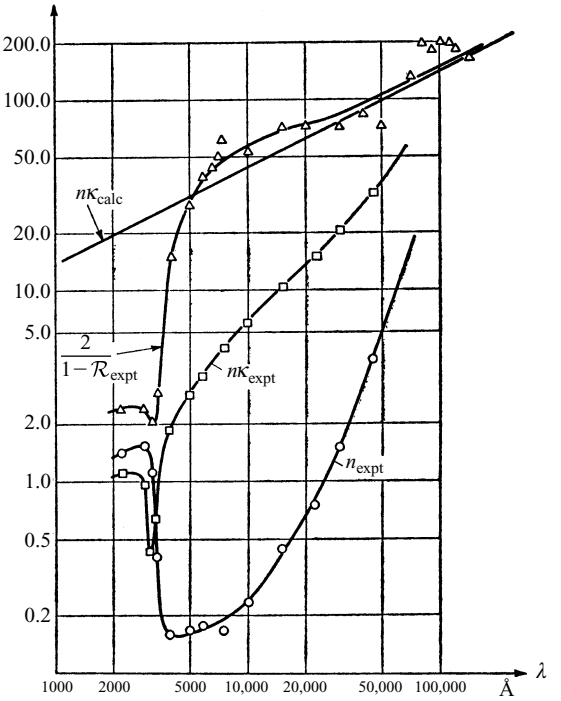

Fig. 14.3 The optical constants of silver as functions of the wavelength. Subscript 'expt' refers to data obtained from experiment. The scales are logarithmic.

$$\mathcal{R} = \frac{2\frac{\sigma}{\nu} + 1 - 2\sqrt{\frac{\sigma}{\nu}}}{2\frac{\sigma}{\nu} + 1 + 2\sqrt{\frac{\sigma}{\nu}}}. \tag{29}$$

When ν/σ is sufficiently small, we may neglect 1 in comparison with the other terms and may develop (29) in powers of $\sqrt{\nu/\sigma}$. We then obtain

$$\mathcal{R} \sim 1 - 2\sqrt{\frac{\nu}{\sigma}} + \cdots. \tag{30}$$

Hagen and Rubens found that, at wavelength $\lambda = 1.2 \times 10^{-3}$ cm, one has for copper $1 - \mathcal{R} = 1.6 \times 10^{-2}$, whilst on substituting for σ the static value of the conductivity, (30) gives $1 - \mathcal{R} = 1.4 \times 10^{-2}$.

As the wavelength is increased further, $\mathcal{R}$ becomes so nearly equal to unity that it is difficult to measure $1 - \mathcal{R}$ with any accuracy. Hagen and Rubens obtained, however, useful estimates by an indirect method. According to *Kirchhoff's law* of heat radiation* the ratio of the emissive power E_ν to the absorptive power A_ν of a body† depends only

* See, for example, M. Planck, *Theory of Heat* (London, Macmillan, 1932), p. 189; or A. Sommerfeld, *Thermodynamics and Statistical Mechanics*, eds. F. Bopp and J. Meixner (New York, Academic Press, 1956), p. 136.

† By emissive power is meant the radiant energy emitted by the body per unit time, by absorptive power the fraction which the body absorbs of the radiant energy which falls upon it.

https://doi.org/10.1017/9781108769914.017 Published online by Cambridge University Press

on the frequency ν and on the temperature T of the body and not on the nature of the body, i.e.

$$\frac{E_\nu}{A_\nu} = K(\nu, T), \tag{31}$$

where $K(\nu, T)$ is a universal function of ν and T. Evidently K is equal to the emissive power of a body whose absorptive power is unity, a so-called *black body*. Now suppose that radiation falls on a metal specimen of such a thickness that all the incident energy that is not reflected is absorbed in its interior. Then

$$A_\nu = 1 - \mathcal{R}, \tag{32}$$

and from (30), (31) and (32)

$$A_\nu = \frac{E_\nu}{K(\nu, T)} = 2\sqrt{\frac{\nu}{\sigma}}, \tag{33}$$

or

$$\sqrt{\sigma}\, E_\nu = 2\sqrt{\nu} K(\nu, T). \tag{34}$$

The right-hand side of this equation is independent of the nature of the metal. It is a well-known function of ν and T, the function $K(\nu, T)$ being precisely known both from experiment and theory, and represented by the celebrated formula of Planck.*

It follows that the validity of the formula (30) may be tested even when $\mathcal{R}$ is very close to unity by determining the conductivity σ and the emissive power E_ν as functions of the frequency and temperature and examining whether the product $\sqrt{\sigma}\, E_\nu$ satisfies (34). Hagen and Rubens confirmed that this is so at long infra-red wavelengths, using for this purpose the so-called *residual rays*. These are rays left over from a wider spectral range after repeated reflections from certain crystals, e.g. fluorite, rock-salt or sylvine. These substances have pronounced absorption maxima in the spectral region $\lambda = 22.9\ \mu$m to $63\ \mu$m, and hence [see (28)] highly selective reflectivity for such wavelengths.

In Fig. 14.3 curves are given, illustrating, for the case of silver, the dependence of n and $n\kappa$ on the wavelength, as determined from experiment. For comparison the theoretical curve computed from the formula §14.1 (24) is also shown. The scales are logarithmic so that the theoretical curve is the straight line

$$\ln n \sim \ln n\kappa \sim \tfrac{1}{2} \ln \lambda + C,$$

where $C = \ln\sqrt{\mu\sigma/c}$. From §14.1 (24) and from (30) we may also express n and $n\kappa$ in terms of the reflectivity (for long waves):

$$n \sim n\kappa \sim \frac{2}{1 - \mathcal{R}}. \tag{35}$$

The function $2/(1 - \mathcal{R})$ is also displayed in the figure for comparison. We see that the experimental curve for $n\kappa$ has a sharp minimum near $\lambda = 3000$ Å and that the curve for n has a much flatter minimum near $\lambda = 5000$ Å. At about $\lambda = 3300$ Å the reflectivity of the silver is seen to be very poor.

* See, for example, M. Born, *Atomic Physics* (London and Glasgow, Blackie and Son, 5th ed., 1951), p. 238.

https://doi.org/10.1017/9781108769914.017 Published online by Cambridge University Press

With increasing wavelength the experimental curves approach the theoretical curve calculated from the conductivity measured electrically.

14.3 Elementary electron theory of the optical constants of metals

We pointed out in the previous sections that the conductivity σ, just as the dielectric constant ε and the magnetic permeability μ, is not a true constant of the medium, but that it depends on the frequency ω of the field. We will now present a rough, simple model (due to P. Drude) from which the frequency dependence of σ may be derived, at least for sufficiently low frequencies.

Let us recall first that the response of a dielectric medium to an external electromagnetic field is largely determined by the behaviour of electrons that are bound to the atomic nuclei by quasi-elastic forces (see §2.3.4). In a conducting medium (such as a metal), unlike in a dielectric, not all the electrons are bound to the atoms. Some move between the molecules and are said to be *free* electrons, to distinguish them from the other electrons that are bound to the atoms, just as in a dielectric. In the absence of an external electromagnetic field, the free electrons move in a random manner and hence they do not give rise to a net current flow. When an external field is applied the free electrons acquire an additional velocity and their motion becomes more orderly, even though occasionally the electrons still collide with the (essentially stationary) atoms. This more orderly motion of the electrons gives rise to the induced current flow.

We cannot enter into a detailed discussion of this process which has to be treated by means of statistical methods of the kinetic theory of gases. The very plausible result is that the averaged total effect is the same as that of a damping force proportional and opposite in direction to the velocity of a model electron that represents the average behaviour of the whole set of electrons. The equation of motion of this model electron in an electric field $\mathbf{E}$ is, therefore,

$$m\ddot{\mathbf{r}} + m\beta\dot{\mathbf{r}} = e\mathbf{E}, \tag{1}$$

where m is the mass, e the charge of the electron and β the damping constant referred to unit mass. Unlike the equation of motion for a bound electron [§2.3 (33)] which contains on the right-hand side an 'effective field' $\mathbf{E}'$, (1) contains on the right-hand side the macroscopic electric field $\mathbf{E}$, which is believed to represent more closely the field that acts on a free electron in a conductor.

In order to understand the meaning of the damping constant β in (1), consider first the case where no electric field is present. If $\mathbf{E} = 0$, we have

$$\ddot{\mathbf{r}} + \beta\dot{\mathbf{r}} = 0, \tag{2}$$

with the solution

$$\mathbf{r} = \mathbf{r}_0 - \frac{1}{\beta}\boldsymbol{v}_0\,\mathrm{e}^{-\beta t}, \qquad \dot{\mathbf{r}} = \boldsymbol{v} = \boldsymbol{v}_0\,\mathrm{e}^{-\beta t}; \tag{3}$$

we see that in this case the model electron starting with the velocity $\boldsymbol{v}_0$ is slowed down in an exponential way, with β as decay constant. The time $\tau = 1/\beta$ is called the *decay time*, or the *relaxation time*. It is typically of the order of 10^{-14} s.

Let us now assume a time-harmonic field $\mathbf{E} = \mathbf{E}_0\,\mathrm{e}^{-\mathrm{i}\omega t}$. The solution of (1) is then

https://doi.org/10.1017/9781108769914.017 Published online by Cambridge University Press

the sum of two terms, one representing the decaying motion [solution of the homogeneous equation (2)] and the other representing a periodic motion

$$\mathbf{r} = -\frac{e}{m(\omega^2 + \mathrm{i}\beta\omega)}\mathbf{E}. \tag{4}$$

This periodic motion gives rise to a current in the medium. If there are N free electrons per unit volume, the current density $\mathbf{j}$ is given by

$$\mathbf{j} = Ne\dot{\mathbf{r}} = \frac{Ne^2}{m(\beta - \mathrm{i}\omega)}\mathbf{E}. \tag{5}$$

Comparing (5) with the constitutive relation §1.1 (9), viz. $\mathbf{j} = \sigma\mathbf{E}$, we see that

$$\sigma = \frac{Ne^2}{m(\beta - \mathrm{i}\omega)}. \tag{6}$$

As we have already mentioned, τ is typically of the order of 10^{-14} s, so that β is then of the order $10^{14}\ \mathrm{s}^{-1}$. It is thus clear, from (6), that when $\omega \ll \beta$, σ may be approximated by its static value $\sigma_0 = Ne^2/m\beta$ which, of course, is real. On the other hand, when $\omega \gg \beta$ (which is usually the case at optical frequencies), the imaginary part of σ will become large compared to its real part. It is, therefore, evident that only for frequencies $\omega \ll \beta$ is one justified in separating the real and imaginary parts of the complex dielectric constant in the manner that leads to the formulae §14.1 (16) and §14.1 (17).

According to §14.1 (16), the frequency dependence of the complex dielectric constant $\hat{\varepsilon}$ and of the complex refractive index $\hat{n}$ arises from the dependence on frequency not only of the conductivity σ (contribution from free electrons), but also of the real dielectric constant ε (contribution from bound electrons). At low enough frequencies the contribution from the bound electrons may be shown to be small compared to the contribution from the free electrons. Under these circumstances we may replace ε by unity and σ by the expression (6) in §14.1 (16). We then obtain, if we assume the conductor to be nonmagnetic ($\mu = 1$), the following expression for $\hat{\varepsilon}$:

$$\hat{\varepsilon} \equiv \hat{n}^2 = 1 - \frac{4\pi Ne^2}{m}\frac{1}{\omega(\omega - \mathrm{i}\beta)}. \tag{7}$$

On separating the real and imaginary parts in (7), and on making use of §14.1 (15a), viz. $\hat{n}^2 = n^2(1 + 2\mathrm{i}\kappa - \kappa^2)$, we obtain the formulae

$$\mathrm{Re}\,\hat{\varepsilon} \equiv n^2(1 - \kappa^2) = 1 - \frac{4\pi Ne^2}{m(\omega^2 + \beta^2)}, \tag{8a}$$

$$\mathrm{Im}\,\hat{\varepsilon} \equiv n^2\kappa = \frac{2\pi Ne^2/\beta}{m\omega(\omega^2 + \beta^2)}. \tag{8b}$$

We may readily deduce from (8a), that if β is sufficiently small, the real part of $\hat{\varepsilon}$ is negative for low enough frequencies, but is evidently positive when ω is large. The critical value ω_c of the frequency at which the real part of $\hat{\varepsilon}$ changes sign is given by

$$\omega_c^2 = \frac{4\pi Ne^2}{m} - \beta^2. \tag{9}$$

We may re-write (8) in terms of this critical value and obtain

https://doi.org/10.1017/9781108769914.017 Published online by Cambridge University Press

$$\operatorname{Re}\hat{\varepsilon} \equiv n^2(1-\kappa^2) = 1 - \frac{\omega_c^2 + \beta^2}{\omega^2 + \beta^2}, \tag{10a}$$

$$\operatorname{Im}\hat{\varepsilon} \equiv n^2\kappa = \frac{\beta(\omega_c^2 + \beta^2)}{2\omega(\omega^2 + \beta^2)}. \tag{10b}$$

We shall now assume that ω_c^2 is much larger than β^2, so that in place of (9) we may write

$$\omega_c^2 \sim \frac{4\pi N e^2}{m}. \tag{11}$$

If we also restrict ourselves to sufficiently high frequencies ($\omega^2 \gg \beta^2$), we obtain, in place of (10), the simpler formulae

$$\operatorname{Re}\hat{\varepsilon} \equiv n^2(1-\kappa^2) \sim 1 - \left(\frac{\omega_c}{\omega}\right)^2, \tag{12a}$$

$$\operatorname{Im}\hat{\varepsilon} \equiv n^2\kappa \sim \frac{\beta}{2\omega}\left(\frac{\omega_c}{\omega}\right)^2. \tag{12b}$$

It follows from (12a) that when $\omega^2 < \omega_c^2$ (but still $\omega^2 \gg \beta^2$), the real part of $\hat{\varepsilon}$ is negative and $\kappa > 1$. The negative value of the real part of $\hat{\varepsilon}$ reflects the fact that under these circumstances the vibrations of the electrons are out of phase by a quarter of a period with the exciting field, as is evident from (5). For sufficiently low values of ω, the attenuation index κ becomes large compared to unity and the reflectivity [given for normal incidence by §14.2 (28)] is readily seen to have a value close to unity. On the other hand, when $\omega^2 > \omega_c^2$ (but $\omega^2 \gg \beta^2$), the real part of $\hat{\varepsilon}$ is evidently positive, so that $\kappa < 1$, and, when ω is sufficiently large, κ becomes small compared to unity and the imaginary part of $\hat{\varepsilon}$ becomes small compared to its real part. The metal must then be expected to behave essentially as a dielectric.

The alkali metals exhibit precisely these phenomena, for in the long wavelength region they are opaque and highly reflecting, whereas at some critical wavelength in the visible or ultra-violet they become transparent, and have comparatively low absorption. Table 14.3 shows in the second row the experimentally determined wavelengths at which this transition occurs. The third row contains these critical wavelengths $\lambda_c = 2\pi c/\omega_c$ determined from the approximate formula (11), where the number of free electrons is taken to be the same as the number N of atoms in the unit volume. It is seen that the values in the two rows are different, except for sodium. The last row gives the ratio of number N_{eff} of electrons that are 'effective' and the number of atoms, determined from the formula

$$\frac{N_{\text{eff}}}{N} = \frac{(\lambda_c)^2_{\text{calc}}}{(\lambda_c)^2_{\text{obs}}}. \tag{13}$$

It is seen that this number is of the order of unity though (except for sodium) considerably smaller. Thus the elementary theory gives the correct order of magnitude of the parameters, but does not describe the phenomena in detail.

The theory can be somewhat improved by using in place of the crude approximations (12) the more accurate formulae (10), which contain the decay constant β. However, because of the complexity of the physical processes involved in the inter-

https://doi.org/10.1017/9781108769914.017 Published online by Cambridge University Press

Table 14.3. *The critical wavelengths λ_c below which the alkali metals become transparent, and above which they are opaque and highly reflecting.*

Metal	Lithium	Sodium	Potassium	Rubidium	Cesium
$(\lambda_c)_{\text{obs}}$	2050 Å	2100 Å	3150 Å	3600 Å	4400 Å
$(\lambda_c)_{\text{calc}}$	1500 Å	2100 Å	2900 Å	3200 Å	3600 Å
$\frac{N_{\text{eff}}}{N}$	0.54	1.00	0.85	0.79	0.67

action of a high-frequency electromagnetic field with a metal, it is not possible to extend appreciably the range of validity of the elementary classical theory that we outlined in this section by a simple modification. A completely satisfactory theory of the optical properties of metals can only be obtained on the basis of quantum mechanics.

14.4 Wave propagation in a stratified conducting medium. Theory of metallic films

In §1.6 we have studied the propagation of electromagnetic waves in stratified dielectric media, that is, in dielectric media with optical properties depending on one Cartesian coordinate only. We shall now briefly discuss the extension of the theory to stratified media that contain absorbing elements. Thus we assume that in addition to ε and μ being functions of only one coordinate, there may be a finite conductivity σ which likewise is a function of this coordinate alone.

As explained at the beginning of §14.2, the formulae of Chapter I as far as they involve only linear relations between the components of the field vectors of a time-harmonic wave retain their validity for conducting media, provided that the real dielectric constant ε and the real wave number k are replaced by the complex dielectric constant $\hat{\varepsilon} = \varepsilon + \mathrm{i}4\pi\sigma/\omega$ and by the complex wave number $\hat{k} = \omega\sqrt{\mu(\varepsilon + \mathrm{i}4\pi\sigma/\omega)}/c$, respectively. Hence we may take over the basic formulae of the theory of stratified dielectric media as developed in §1.6, provided we make this formal change in the appropriate formulae. It follows, in particular, that a stratified absorbing medium may be characterized by a two-by-two matrix. In contrast to the case of a dielectric stratified medium, the elements of this matrix are no longer real or pure imaginary numbers but are complex numbers that contain both real and imaginary parts.

We shall illustrate the theory by studying in detail two cases of practical interest.

14.4.1 An absorbing film on a transparent substrate

Consider a plane-parallel absorbing film situated between two dielectric media (Fig. 14.4). The formulae relating to the reflection and transmission of a plane monochromatic wave by the film are obtained from §1.6 (55)–(58) on replacing n_2 by $\hat{n}_2 = n_2(1 + \mathrm{i}\kappa_2)$. It is convenient to set

$$\hat{n}_2 \cos\theta_2 = u_2 + \mathrm{i}v_2, \tag{1}$$

https://doi.org/10.1017/9781108769914.017 Published online by Cambridge University Press

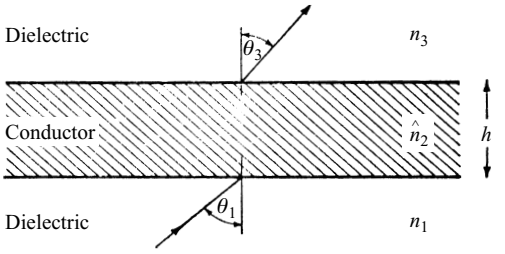

Fig. 14.4 An absorbing film situated between two dielectric media.

where u_2 and v_2 are real. We can easily express u_2 and v_2 in terms of the angle of incidence and the constants which characterize the optical properties of the first and the second medium. It follows, on squaring (1) and using the law of refraction $\hat{n}_2 \sin\theta_2 = n_1 \sin\theta_1$, that

$$(u_2 + \mathrm{i}v_2)^2 = \hat{n}_2^2 - n_1^2 \sin^2\theta_1. \tag{2}$$

On equating real and imaginary parts this gives

$$\left.\begin{aligned} u_2^2 - v_2^2 &= n_2^2(1-\kappa_2^2) - n_1^2 \sin^2\theta_1, \\ u_2 v_2 &= n_2^2 \kappa_2. \end{aligned}\right\} \tag{3}$$

From (3) we find that

$$\left.\begin{aligned} 2u_2^2 &= n_2^2(1-\kappa_2^2) - n_1^2 \sin^2\theta_1 + \sqrt{[n_2^2(1-\kappa_2^2) - n_1^2 \sin^2\theta_1]^2 + 4n_2^4\kappa_2^2}, \\ 2v_2^2 &= -[n_2^2(1-\kappa_2^2) - n_1^2 \sin^2\theta_1] + \sqrt{[n_2^2(1-\kappa_2^2) - n_1^2 \sin^2\theta_1]^2 + 4n_2^4\kappa_2^2}. \end{aligned}\right\} \tag{4}$$

Next we must evaluate the reflection and transmission coefficients for the interfaces 1–2 and 2–3 respectively, for these coefficients enter the formulae for the reflection and transmission coefficients of the film. We consider separately the cases when the electric vector of the incident wave is perpendicular, or parallel, to the plane of incidence.

Electric vector perpendicular to the plane of incidence (TE wave)

In this case we have, on replacing $n_2 \cos\theta_2$ by $\hat{n}_2 \cos\theta_2 = u_2 + \mathrm{i}v_2$ in §1.6 (55),

$$r_{12} = \rho_{12}\, \mathrm{e}^{\mathrm{i}\phi_{12}} = \frac{n_1 \cos\theta_1 - (u_2 + \mathrm{i}v_2)}{n_1 \cos\theta_1 + (u_2 + \mathrm{i}v_2)}. \tag{5}$$

We shall later need explicit expressions for the amplitude ρ_{12} and the phase change ϕ_{12}. From (5) we have:

$$\rho_{12}^2 = \frac{(n_1 \cos\theta_1 - u_2)^2 + v_2^2}{(n_1 \cos\theta_1 + u_2)^2 + v_2^2}, \qquad \tan\phi_{12} = \frac{2v_2 n_1 \cos\theta_1}{u_2^2 + v_2^2 - n_1^2 \cos^2\theta_1}. \tag{6}$$

For transmission at the first interface, we have from §1.6 (56)

https://doi.org/10.1017/9781108769914.017 Published online by Cambridge University Press

$$t_{12} = \tau_{12}\,\mathrm{e}^{\mathrm{i}\chi_{12}} = \frac{2n_1\cos\theta_1}{n_1\cos\theta_1 + u_2 + \mathrm{i}v_2}, \tag{7}$$

which gives

$$\tau_{12}^2 = \frac{(2n_1\cos\theta_1)^2}{(n_1\cos\theta_1 + u_2)^2 + v_2^2}, \qquad \tan\chi_{12} = -\frac{v_2}{n_1\cos\theta_1 + u_2}. \tag{8}$$

In a strictly analogous way we obtain the following expressions relating to reflection and transmission at the second interface:

$$\rho_{23}^2 = \frac{(n_3\cos\theta_3 - u_2)^2 + v_2^2}{(n_3\cos\theta_3 + u_2)^2 + v_2^2}, \qquad \tan\phi_{23} = \frac{2v_2 n_3\cos\theta_3}{u_2^2 + v_2^2 - n_3^2\cos^2\theta_3}, \tag{9}$$

$$\tau_{23}^2 = \frac{4(u_2^2 + v_2^2)}{(n_3\cos\theta_3 + u_2)^2 + v_2^2}, \qquad \tan\chi_{23} = \frac{v_2 n_3\cos\theta_3}{u_2^2 + v_2^2 + u_2 n_3\cos\theta_3}. \tag{10}$$

Since, according to the law of refraction $n_1\sin\theta_1 = \hat{n}_2\sin\theta_2$, $\hat{n}_2\sin\theta_2 = n_3\sin\theta_3$, the angle θ_3 is determined from θ_1 by means of the formula

$$n_3\sin\theta_3 = n_1\sin\theta_1. \tag{11}$$

Electric vector parallel to the plane of incidence (TM wave)

As explained in §1.6.3 the formulae for the reflection and transmission coefficients for a TM wave can be obtained from those for a TE wave simply by replacing the quantities $p_j = n_j\cos\theta_j$ by $q_j = \cos\theta_j/n_j$, it being assumed that the media are nonmagnetic. The quantities r and t now refer to the ratios of the magnetic, not the electric vectors. In particular we have from §1.6 (55),

$$\begin{aligned} r_{12} = \rho_{12}\,\mathrm{e}^{\mathrm{i}\phi_{12}} &= \frac{\dfrac{1}{n_1}\cos\theta_1 - \dfrac{1}{\hat{n}_2}\cos\theta_2}{\dfrac{1}{n_1}\cos\theta_1 + \dfrac{1}{\hat{n}_2}\cos\theta_2} = \frac{\hat{n}_2^2\cos\theta_1 - n_1\hat{n}_2\cos\theta_2}{\hat{n}_2^2\cos\theta_1 + n_1\hat{n}_2\cos\theta_2} \\ &= \frac{[n_2^2(1-\kappa_2^2) + 2in_2^2\kappa_2]\cos\theta_1 - n_1(u_2 + \mathrm{i}v_2)}{[n_2^2(1-\kappa_2^2) + 2in_2^2\kappa_2]\cos\theta_1 + n_1(u_2 + \mathrm{i}v_2)}. \end{aligned} \tag{12}$$

From (12) we find after a straightforward calculation

$$\left.\begin{aligned} \rho_{12}^2 &= \frac{[n_2^2(1-\kappa_2^2)\cos\theta_1 - n_1u_2]^2 + [2n_2^2\kappa_2\cos\theta_1 - n_1v_2]^2}{[n_2^2(1-\kappa_2^2)\cos\theta_1 + n_1u_2]^2 + [2n_2^2\kappa_2\cos\theta_1 + n_1v_2]^2}, \\ \tan\phi_{12} &= 2n_1n_2^2\cos\theta_1\,\frac{2\kappa_2u_2 - (1-\kappa_2^2)v_2}{n_2^4(1+\kappa_2^2)^2\cos^2\theta_1 - n_1^2(u_2^2 + v_2^2)}. \end{aligned}\right\} \tag{13}$$

For the ratio t_{12} we obtain from §1.6 (56) on replacing $n_j\cos\theta_j$ by $\cos\theta_j/n_j$,

https://doi.org/10.1017/9781108769914.017 Published online by Cambridge University Press

$$t_{12} = \tau_{12}\,\mathrm{e}^{\mathrm{i}\chi_{12}} = \frac{\dfrac{2}{n_1}\cos\theta_1}{\dfrac{1}{n_1}\cos\theta_1 + \dfrac{1}{\hat{n}_2}\cos\theta_2}$$

$$= \frac{2[n_2^2(1-\kappa_2^2) + 2in_2^2\kappa_2]\cos\theta_1}{[n_2^2(1-\kappa_2^2) + 2in_2^2\kappa_2]\cos\theta_1 + n_1(u_2 + \mathrm{i}v_2)}. \tag{14}$$

From (14) we find that

$$\left.\begin{aligned} \tau_{12}^2 &= \frac{4n_2^4(1+\kappa_2^2)^2\cos^2\theta_1}{[n_2^2(1-\kappa_2^2)\cos\theta_1 + n_1u_2]^2 + (2n_2^2\kappa_2\cos\theta_1 + n_1v_2)^2}, \\ \tan\chi_{12} &= \frac{n_1[2\kappa_2u_2 - (1-\kappa_2^2)v_2]}{n_2^2(1+\kappa_2^2)^2\cos\theta_1 + n_1[(1-\kappa_2^2)u_2 + 2\kappa_2v_2]}. \end{aligned}\right\} \tag{15}$$

In a similar way we obtain the following formulae for the reflection and transmission coefficients relating to the second interface:

$$\left.\begin{aligned} \rho_{23}^2 &= \frac{[n_2^2(1-\kappa_2^2)\cos\theta_3 - n_3u_2]^2 + [2n_2^2\kappa_2\cos\theta_3 - n_3v_2]^2}{[n_2^2(1-\kappa_2^2)\cos\theta_3 + n_3u_2]^2 + [2n_2^2\kappa_2\cos\theta_3 + n_3v_2]^2}, \\ \tan\phi_{23} &= 2n_3n_2^2\cos\theta_3\,\frac{2\kappa_2u_2 - (1-\kappa_2^2)v_2}{n_2^4(1+\kappa_2^2)^2\cos^2\theta_3 - n_3^2(u_2^2+v_2^2)}, \end{aligned}\right\} \tag{16}$$

and

$$\left.\begin{aligned} \tau_{23}^2 &= \frac{4n_3^2(u_2^2+v_2^2)}{[n_3u_2 + n_2^2(1-\kappa_2^2)\cos\theta_3]^2 + (n_3v_2 + 2n_2^2\kappa_2\cos\theta_3)^2}, \\ \tan\chi_{23} &= \frac{n_2^2[(1-\kappa_2)^2v_2 - 2\kappa_2u_2]\cos\theta_3}{n_3(u_2^2+v_2^2) + n_2^2[(1-\kappa_2)^2u_2 + 2\kappa_2v_2]\cos\theta_3}. \end{aligned}\right\} \tag{17}$$

From the knowledge of the quantities ρ_{12}, ϕ_{12}, etc., the complex reflection and transmission coefficients of the film may immediately be evaluated. It will be useful to set

$$\eta = \frac{2\pi}{\lambda_0}h, \tag{18}$$

so that

$$\beta = \frac{2\pi}{\lambda_0}\hat{n}_2h\cos\theta_2 = (u_2 + \mathrm{i}v_2)\eta. \tag{19}$$

The equations §1.6 (57)–(58) now become

$$r = \rho\mathrm{e}^{\mathrm{i}\delta_r} = \frac{\rho_{12}\,\mathrm{e}^{\mathrm{i}\phi_{12}} + \rho_{23}\,\mathrm{e}^{-2v_2\eta}\,\mathrm{e}^{\mathrm{i}(\phi_{23}+2u_2\eta)}}{1 + \rho_{12}\rho_{23}\,\mathrm{e}^{-2v_2\eta}\,\mathrm{e}^{\mathrm{i}(\phi_{12}+\phi_{23}+2u_2\eta)}}, \tag{20}$$

$$t = \tau\mathrm{e}^{\mathrm{i}\delta_t} = \frac{\tau_{12}\tau_{23}\,\mathrm{e}^{-v_2\eta}\,\mathrm{e}^{\mathrm{i}(\chi_{12}+\chi_{23}+u_2\eta)}}{1 + \rho_{12}\rho_{23}\,\mathrm{e}^{-2v_2\eta}\,\mathrm{e}^{\mathrm{i}(\phi_{12}+\phi_{23}+2u_2\eta)}}. \tag{21}$$

https://doi.org/10.1017/9781108769914.017 Published online by Cambridge University Press

From (20) we obtain, after straightforward calculation, the following expressions for the reflectivity $\mathcal{R}$ and for the phase change δ_r on reflection:

$$\mathcal{R} = |r|^2 = \frac{\rho_{12}^2 \, \mathrm{e}^{2v_2\eta} + \rho_{23}^2 \, \mathrm{e}^{-2v_2\eta} + 2\rho_{12}\rho_{23}\cos(\phi_{23} - \phi_{12} + 2u_2\eta)}{\mathrm{e}^{2v_2\eta} + \rho_{12}^2\rho_{23}^2 \, \mathrm{e}^{-2v_2\eta} + 2\rho_{12}\rho_{23}\cos(\phi_{12} + \phi_{23} + 2u_2\eta)}, \tag{22}$$

$$\tan\delta_r = \frac{\rho_{23}(1 - \rho_{12}^2)\sin(2u_2\eta + \phi_{23}) + \rho_{12}(\mathrm{e}^{2v_2\eta} - \rho_{23}^2 \, \mathrm{e}^{-2v_2\eta})\sin\phi_{12}}{\rho_{23}(1 + \rho_{12}^2)\cos(2u_2\eta + \phi_{23}) + \rho_{12}(\mathrm{e}^{2v_2\eta} + \rho_{23}^2 \, \mathrm{e}^{-2v_2\eta})\cos\phi_{12}}. \tag{23}$$

These formulae are valid for a TE wave as well as for a TM wave. In the former case one must substitute for ρ and ϕ the values given by (6) and (9), in the latter case those given by (13) and (16).

In a similar way we obtain from (21) the following expressions for the transmissivity $\mathcal{T}$ and for the phase change δ_t on transmission:

$$\begin{aligned} \mathcal{T} &= \frac{n_3\cos\theta_3}{n_1\cos\theta_1}|t|^2 \\ &= \frac{n_3\cos\theta_3}{n_1\cos\theta_1}\frac{\tau_{12}^2\tau_{23}^2 \, \mathrm{e}^{-2v_2\eta}}{1 + \rho_{12}^2\rho_{23}^2 \, \mathrm{e}^{-4v_2\eta} + 2\rho_{12}\rho_{23} \, \mathrm{e}^{-2v_2\eta}\cos(\phi_{12} + \phi_{23} + 2u_2\eta)}, \end{aligned} \tag{24}$$

$$\tan[\delta_t - \chi_{12} - \chi_{23} + u_2\eta] = \frac{\mathrm{e}^{2v_2\eta}\sin 2u_2\eta - \rho_{12}\rho_{23}\sin(\phi_{12} + \phi_{23})}{\mathrm{e}^{2v_2\eta}\cos 2u_2\eta + \rho_{12}\rho_{23}\cos(\phi_{12} + \phi_{23})}. \tag{25}$$

For a TM wave the factor $n_3\cos\theta_3/n_1\cos\theta_1$ must be replaced by $(\cos\theta_3/n_3)/(\cos\theta_1/n_1)$. For a TE wave the values given by (6), (8), (9) and (10) are substituted in these formulae, and for a TM wave those given by (13), (15), (16) and (17).

It may be worthwhile to recall that the phase change on reflection (δ_r) is referred to the first boundary (1–2), whereas the phase change on transmission (δ_t) is referred to the second boundary.

Eqs. (22)–(25) allow the computations of the four basic quantities that characterize reflection and transmission by an absorbing film of known optical properties and of prescribed thickness. Fig. 14.5 illustrates, for some typical cases, the dependence of the reflectivity and transmissivity on the thickness of the film.

For a nonabsorbing film $\mathcal{R}$ and $\mathcal{T}$ are periodic functions of the film thickness h, with a period of one wavelength. Absorption is seen to reduce the amplitude of the successive maxima and to give rise to a displacement of the maxima in the direction of smaller thickness. At optical wavelengths absorption of metals is so large that the thickness at which there is appreciable transmission is well below a quarter wavelength* (see Table 14.1, p. 739). With transmitted light maxima and minima are therefore not observed.

In optics, metal films are chiefly used to attain high reflectivities, for example in connection with the Fabry–Perot interferometer (§7.6.2). Such films used to be

* Simplified formulae relating to such thin films may be obtained by expanding the numerator and denominator (22)–(25) into series in powers of the film thickness, and retaining terms in the first few powers only (see F. Abelès, *Rev. d'Optique*, **32** (1953), 257).

The optical properties of thin metallic films in the visible and infra-red spectral region are thoroughly discussed by L. N. Hadley and D. M. Dennison, *J. Opt. Soc. Amer.*, **37** (1947), 451; **38** (1948), 483.

https://doi.org/10.1017/9781108769914.017 Published online by Cambridge University Press

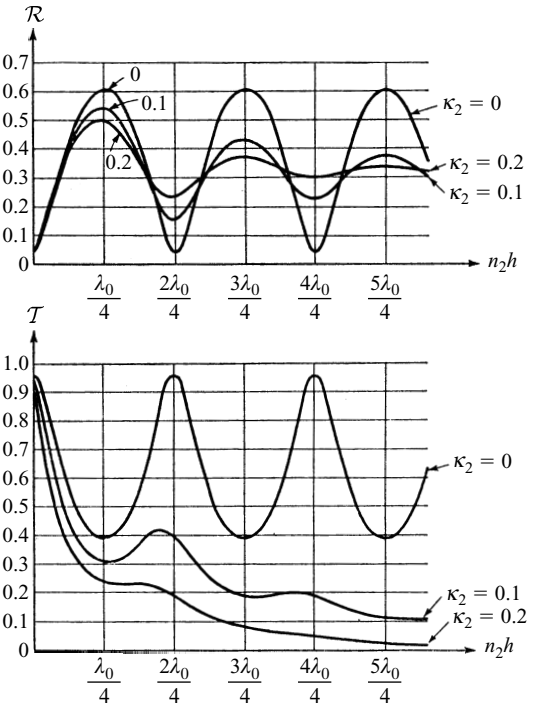

Fig. 14.5 The reflectivity $\mathcal{R}$ and transmissivity $\mathcal{T}$ of a metallic film as functions of its optical thickness. [$n_1 = 1$, $n_2 = 3.5$, $n_3 = 1.5$, $\kappa_1 = \kappa_3 = 0$; $\theta_1 = 0$.] (After K. Hammer, *Z. Tech. Phys.*, **24** (1943), 169.)

produced by chemical deposition but this method has in more recent times been superseded by the techniques of high-vacuum evaporation.*

Finally let us briefly consider reflection and transmission with a 'thick' film. If the thickness h and consequently the parameter η are sufficiently large all the terms in (22)–(25) which do not contain the multiplicative factor $\exp(2v_2\eta)$ may be neglected. For example, if $\exp(2v_2\eta) \geqslant 100$ this neglect does not, as a rule, involve an error of more than a few per cent. For such a film, one has at normal incidence $4\pi h n_2\kappa_2/\lambda \geqslant \ln 100 = 4.61$, or (dropping the suffix 2),

$$\frac{h}{\lambda} \geqslant \frac{0.37}{n\kappa}. \tag{26}$$

For a silver film, for example, $n\kappa \sim 3.67$ at $\lambda = 5780$ Å, and (26) gives $h \geqslant \lambda/10 \sim 5.8 \times 10^{-6}$ cm.

For a thick film, we have from (22) and (24)

$$\mathcal{R} \sim \rho_{12}^2, \qquad \mathcal{T} = \frac{n_3 \cos\theta_3}{n_1 \cos\theta_1} \tau_{12}^2 \tau_{23}^2 \, \mathrm{e}^{-4v_2\eta}. \tag{27}$$

We see that the reflectivity of a 'thick' film is almost that of an infinitely thick one, and

* See, for example, S. Tolansky, *Multiple-beam Interferometry of Surfaces and Films* (Oxford, Oxford University Press, 1948), p. 26; or O. S. Heavens, *Optical Properties of Thin Solid Films* (London, Butterworths, 1955).

https://doi.org/10.1017/9781108769914.017 Published online by Cambridge University Press

that its transmissivity decreases exponentially with the thickness. The phase changes are immediately obtained from (23) and (25):

$$\delta_r \sim \phi_{12}, \qquad \delta \sim \chi_{12} + \chi_{23} + u_2\eta. \tag{28}$$

Formulae (27) and (28) interpret our definition of a 'thick' film in somewhat more physical terms, implying that in such a film the effect of multiple beam interference is negligible.

14.4.2 A transparent film on an absorbing substrate

As a second example, consider reflection from a transparent film on an absorbing substrate (Fig. 14.6).

In this case r_{12} is real whilst r_{23} is complex. The amplitude ratio ρ_{23} and the phase change ϕ_{23} are given by (6) or (13), with suffixes 1 and 2 replaced by 2 and 3 respectively. According to §1.6 (57) we now have

$$r = \frac{r_{12} + \rho_{23}\, e^{i(\phi_{23}+2\beta)}}{1 + r_{12}\rho_{23}\, e^{i(\phi_{23}+2\beta)}}. \tag{29}$$

This expression is identical with §1.6 (57) if 2β is replaced by $2\beta + \phi_{23}$ and r_{23} by ρ_{23}. Thus without any calculation we may at once write down the expression for the reflectivity and the phase change on reflection, simply by making this substitution in §1.6 (59) and §1.6 (61); we then obtain

$$\mathcal{R} = \frac{r_{12}^2 + \rho_{23}^2 + 2r_{12}\rho_{23}\cos(\phi_{23} + 2\beta)}{1 + r_{12}^2\rho_{23}^2 + 2r_{12}\rho_{23}\cos(\phi_{23} + 2\beta)}, \tag{30}$$

and

$$\tan\delta_r = \frac{\rho_{23}(1 - r_{12}^2)\sin(\phi_{23} + 2\beta)}{r_{12}(1 + \rho_{23}^2) + \rho_{23}(1 + r_{12}^2)\cos(\phi_{23} + 2\beta)}. \tag{31}$$

Thin transparent films on absorbing substrates have many practical uses. They are employed, for example, to protect metallic mirrors and to increase their reflectivity. They may also be used to reduce the reflectivity of a metal surface. We have mentioned on p. 68 that one may design a polarizer consisting of a dielectric film on a dielectric substrate for which $\mathcal{R}_\parallel = 0$ and $\mathcal{R}_\perp$ is quite large. With a metallic substrate one may have either* $\mathcal{R}_\parallel = 0$ or $\mathcal{R}_\perp = 0$.

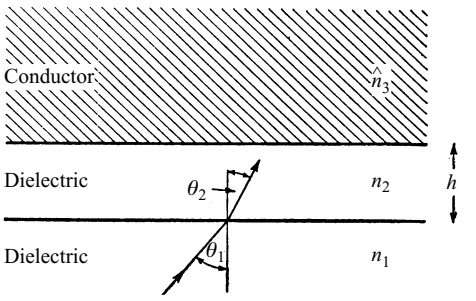

Fig. 14.6 A transparent film on an absorbing substrate.

* See H. Schopper, *Optik*, **10** (1953), 426.

https://doi.org/10.1017/9781108769914.017 Published online by Cambridge University Press

14.5 Diffraction by a conducting sphere; theory of Mie

Metals exhibit marked optical characteristics not only in bulk, but also when they are finely divided, as in colloidal suspensions. We may recall the brilliant ruby colours of colloidal gold, whether in liquids or glasses. These phenomena are of great interest, as refraction, absorption and diffraction take place here side by side.

Were the metallic particles perfect conductors, one would be dealing with a problem of pure diffraction. We have, however, not discussed the subject from this standpoint in the chapters on diffraction, since it is the effects that are due to partial penetration of light into the particles that are of particular physical interest. Absorption then plays an important part and it is, therefore, more appropriate to treat the subject in the present chapter; the corresponding results relating to dielectric spheres are contained in our considerations as a limiting case ($\kappa \to 0$).

Of the early workers who studied the optical properties of metallic particles, mention must be made of Maxwell Garnett.* He considered the passage of light through a dielectric medium containing many small metallic spheres in a volume of linear dimensions of a wavelength. With the help of the Lorentz–Lorenz formula [§2.3 (17)] Maxwell Garnett showed that such an assembly is equivalent to a medium of a certain complex refractive index $\hat{n}' = n'(1 + \mathrm{i}\kappa')$ and he found formulae for n' and κ' in terms of the indices n and κ that characterize the metallic spheres. By means of these considerations he was able to account for some of the observed features.

In a paper published in 1908, G. Mie† obtained, on the basis of the electromagnetic theory, a rigorous solution for the diffraction of a plane monochromatic wave by a homogeneous sphere of any diameter and of any composition situated in a homogeneous medium. An equivalent solution of the same problem was published shortly afterwards by P. Debye‡ in a paper concerned with light pressure (i.e. the mechanical force exerted by light) on a conducting sphere, and since then the subject has been treated in its different aspects by many writers.§

The solution due to Mie, though derived for diffraction by a single sphere, also applies to diffraction by any number of spheres, provided that they are all of the same diameter and composition and provided also that they are randomly distributed and separated from each other by distances that are large compared to the wavelength. Under these circumstances there are no coherent phase relationships between the light that is scattered by the different spheres and the total scattered energy is then equal to the energy that is scattered by one sphere multiplied by their total number. It is particularly in this connection that Mie's solution is of great practical value and may be applied to a variety of problems: in addition to the question of colours exhibited by metallic suspensions, we may mention applications such as the study of atmospheric dust, interstellar particles or colloidal suspensions, the theory of the rainbow, the solar corona, the effects of clouds and fogs on the transmission of light, etc.‖

* J. C. Maxwell Garnett, *Phil. Trans. Roy. Soc.*, A, **203**, (1904), 385; *ibid*. **205** (1906), 237.

† G. Mie, *Ann. d. Physik* (4), **25** (1908), 377. ‡ P. Debye, *Ann. d. Physik* (4), **30** (1909), 57.

§ Of later investigations that deal with the basic theory, particular mention may be made of contributions by T. J. I'A. Bromwich, *Phil. Trans. Roy. Soc.*, A, **220** (1920), 175 and by H. C. van de Hulst, *Rech. Astron. Observ. Utrecht*, XI, Pt. 1 (1946).

‖ For an account of some of these topics and of more recent developments in the theory see H. M. Nussenzveig, *Diffraction Effects in Semiclassical Scattering* (Cambridge, Cambridge University Press, 1992).

Before deriving Mie's formulae it will be helpful to explain briefly the method employed. We are concerned with finding the solution of Maxwell's equations which describe the field arising from a plane monochromatic wave incident upon a spherical surface, across which the properties of the medium change abruptly. An appropriate system of curvilinear coordinates (spherical polar coordinates) is introduced and the field is represented as the sum of two 'subfields'; one of the subfields is such that its electric vector has no radial component while the other has a magnetic vector with this property. In spherical polar coordinates Maxwell's equations together with the boundary conditions separate into a set of ordinary differential equations, which are then solved for the two subfields in the form of infinite series. §14.5.1 is concerned with the derivation of this solution and in §14.5.2 the main consequences of the solution are discussed. The final section (§14.5.3) is concerned with some general results relating to the total amount of energy that is scattered and absorbed by an obstacle of arbitrary shape, and the case of a spherical obstacle is discussed in detail.

14.5.1 Mathematical solution of the problem

(a) Representation of the field in terms of Debye's potentials

We consider the diffraction of a plane, linearly polarized, monochromatic wave by a sphere of radius a, immersed in a homogeneous, isotropic medium. We assume that the medium in which the sphere is embedded is a nonconductor and that both this medium as well as the sphere are non-magnetic.

Assuming, as usual, the time dependence $\exp(-\mathrm{i}\omega t)$, the time-independent parts of the electric and magnetic vectors both outside and inside the sphere satisfy Maxwell's equations in their time-free form:

$$\left.\begin{aligned} \operatorname{curl}\mathbf{H} &= -k_1\mathbf{E}, \qquad \text{(a)} \\ \operatorname{curl}\mathbf{E} &= \quad k_2\mathbf{H}, \qquad \text{(b)} \end{aligned}\right\} \tag{1}$$

where

$$\left.\begin{aligned} k_1 &= \frac{\mathrm{i}\omega}{c}\left(\varepsilon + \mathrm{i}\frac{4\pi\sigma}{\omega}\right), \qquad \text{(a)} \\ k_2 &= \frac{\mathrm{i}\omega}{c}. \qquad \text{(b)} \end{aligned}\right\} \tag{2}$$

The square of the usual wave number k (real outside and complex inside the sphere) is

$$k^2 = -k_1 k_2. \tag{3}$$

Quantities which refer to the medium surrounding the sphere will be denoted by superscript I, those referring to the sphere by superscript II. As the medium surrounding the sphere is assumed to be non-conducting, $\sigma^{(\mathrm{I})} = 0$.

We take a rectangular system of coordinates with origin at the centre of the sphere with the z direction in the direction of propagation of the wave and with the x direction in the direction of its electric vector (Fig. 14.7). If the amplitude of the electric vector of the incident wave is normalized to unity, i.e.

$$|\mathbf{E}^{(i)}| = |\mathrm{e}^{\mathrm{i}k^{(\mathrm{I})}z}| = 1,$$

https://doi.org/10.1017/9781108769914.017 Published online by Cambridge University Press

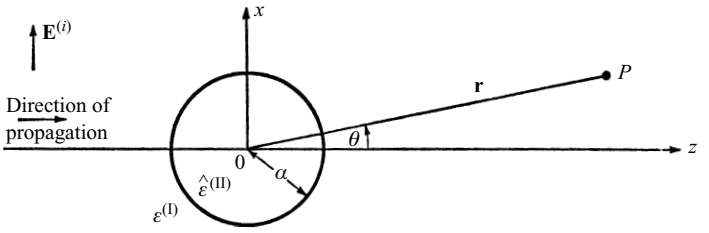

Fig. 14.7 Diffraction by a conducting sphere: notation.

the six components of the field vectors are

$$\left.\begin{aligned} E_x^{(i)} &= \mathrm{e}^{\mathrm{i}k^{(\mathrm{I})}z}, \\ H_y^{(i)} &= \frac{\mathrm{i}k^{(\mathrm{I})}}{k_2^{(\mathrm{I})}}\,\mathrm{e}^{\mathrm{i}k^{(\mathrm{I})}z}, \\ E_y^{(i)} &= E_z^{(i)} = H_x^{(i)} = H_z^{(i)} = 0. \end{aligned}\right\} \tag{4}$$

As regards boundary conditions, we only demand, in accordance with §1.1.3, that the tangential components of $\mathbf{E}$ and $\mathbf{H}$ shall be continuous across the surface of the sphere:

$$\left.\begin{aligned} E_{\mathrm{tang}}^{(\mathrm{I})} &= E_{\mathrm{tang}}^{(\mathrm{II})}, \\ H_{\mathrm{tang}}^{(\mathrm{I})} &= H_{\mathrm{tang}}^{(\mathrm{II})}, \end{aligned}\right\} \quad \text{when } r = a. \tag{5}$$

The condition that the radial components of $\varepsilon\mathbf{E}$ and $\mathbf{H}$ shall also be continuous across the surface then follows from (5) and from Maxwell's equations.

In order to satisfy the boundary conditions, we must assume that apart from the incident field $\mathbf{E}^{(i)}$, $\mathbf{H}^{(i)}$ and the field $\mathbf{E}^{(w)}$, $\mathbf{H}^{(w)}$ within the sphere there is a secondary (scattered or diffracted) field $\mathbf{E}^{(s)}$, $\mathbf{H}^{(s)}$ in the medium surrounding the sphere. Thus the total electric field in the two regions is written as

$$\left.\begin{aligned} \mathbf{E} &= \mathbf{E}^{(i)} + \mathbf{E}^{(s)} \quad \text{outside the sphere}, \\ &= \mathbf{E}^{(w)} \qquad\quad \text{within the sphere}, \end{aligned}\right\} \tag{6}$$

with similar expressions for the magnetic vector. The fields $\mathbf{E}^{(s)}$, $\mathbf{H}^{(s)}$ and $\mathbf{E}^{(w)}$, $\mathbf{H}^{(w)}$ may be considered to be analogous to the reflected field and the transmitted field respectively, for propagation involving a plane boundary (§1.5.1); this analogy is, however, appropriate only when the diameter of the sphere is large compared with the wavelength. Since the boundary conditions must hold for all time, all the six vectors must have the same time dependence [$\exp(-\mathrm{i}\omega t)$].

The curvilinear coordinates appropriate to the present problem are the spherical polar coordinates, r, θ and ϕ defined by

$$\left.\begin{aligned} x &= r\sin\theta\cos\phi, \\ y &= r\sin\theta\sin\phi, \\ z &= r\cos\theta. \end{aligned}\right\} \tag{7}$$

https://doi.org/10.1017/9781108769914.017 Published online by Cambridge University Press

The components of any vector **A** are transformed from the Cartesian system to this new system according to the rule*

$$\left.\begin{aligned} A_r &= A_x \sin\theta\cos\phi + A_y \sin\theta\sin\phi + A_z\cos\theta, \\ A_\theta &= A_x\cos\theta\cos\phi + A_y\cos\theta\sin\phi - A_z\sin\theta, \\ A_\phi &= -A_x\sin\phi + A_y\cos\phi. \end{aligned}\right\} \tag{8}$$

Applying these formulae to the vector curl **A** we obtain

$$\left.\begin{aligned} (\operatorname{curl}\mathbf{A})_r &= \frac{1}{r^2\sin\theta}\left[\frac{\partial(rA_\phi\sin\theta)}{\partial\theta} - \frac{\partial(rA_\theta)}{\partial\phi}\right], \\ (\operatorname{curl}\mathbf{A})_\theta &= \frac{1}{r\sin\theta}\left[\frac{\partial A_r}{\partial\phi} - \frac{\partial(rA_\phi\sin\theta)}{\partial r}\right], \\ (\operatorname{curl}\mathbf{A})_\phi &= \frac{1}{r}\left[\frac{\partial(rA_\theta)}{\partial r} - \frac{\partial A_r}{\partial\theta}\right]. \end{aligned}\right\} \tag{9}$$

In the spherical polar coordinates, the field equations (1) become

$$\left.\begin{aligned} -k_1E_r &= \frac{1}{r^2\sin\theta}\left[\frac{\partial(rH_\phi\sin\theta)}{\partial\theta} - \frac{\partial(rH_\theta)}{\partial\phi}\right], && (\alpha) \\ -k_1E_\theta &= \frac{1}{r\sin\theta}\left[\frac{\partial H_r}{\partial\phi} - \frac{\partial(rH_\phi\sin\theta)}{\partial r}\right], && (\beta) \\ -k_1E_\phi &= \frac{1}{r}\left[\frac{\partial(rH_\theta)}{\partial r} - \frac{\partial H_r}{\partial\theta}\right]. && (\gamma) \end{aligned}\right\} \text{(a)}$$

$$\left.\begin{aligned} k_2H_r &= \frac{1}{r^2\sin\theta}\left[\frac{\partial(rE_\phi\sin\theta)}{\partial\theta} - \frac{\partial(rE_\theta)}{\partial\phi}\right], && (\alpha) \\ k_2H_\theta &= \frac{1}{r\sin\theta}\left[\frac{\partial E_r}{\partial\phi} - \frac{\partial(rE_\phi\sin\theta)}{\partial r}\right], && (\beta) \\ k_2H_\phi &= \frac{1}{r}\left[\frac{\partial(rE_\theta)}{\partial r} - \frac{\partial E_r}{\partial\theta}\right]. && (\gamma) \end{aligned}\right\} \text{(b)} \tag{10}$$

* See, for example, W. Magnus and F. Oberhettinger, *Formulas and Theorems for the Functions of Mathematical Physics* (New York, Chelsea Publishing Company, 1954), p. 146.

The components defined here are not those employed in the absolute differential calculus of Ricci and Levi-Civita. There one has two sets of different but equivalent components of a vector **A**, the contravariant components A^i and the covariant components A_i. If $\mathbf{e}_1$, $\mathbf{e}_2$ and $\mathbf{e}_3$ are base vectors, in general nonorthogonal and of different lengths, the contravariant components (with respect to these base vectors) may be defined as the coefficients in the representation $\mathbf{A} = A^1\mathbf{e}_1 + A^2\mathbf{e}_2 + A^3\mathbf{e}_3$; and the covariant components may be defined as the coefficients in the representation $\mathbf{A} = A_1\mathbf{e}^1 + A_2\mathbf{e}^2 + A_3\mathbf{e}^3$, where $\mathbf{e}^1$, $\mathbf{e}^2$ and $\mathbf{e}^3$ are the reciprocal vectors, i.e. vectors satisfying the relations $\mathbf{e}^i\cdot\mathbf{e}_k = \delta_{ik}$, where δ_{ik} is the Kronecker symbol. In the special case when $\mathbf{e}_1$, $\mathbf{e}_2$ and $\mathbf{e}_3$ are orthogonal, so are also $\mathbf{e}^1$, $\mathbf{e}^2$ and $\mathbf{e}^3$ and the corresponding vectors in the two sets are parallel. One can then introduce one set of *natural* components $\overline{A}_i = \sqrt{A_iA^i}$ and these have a simple geometrical interpretation: they are the orthogonal projections of **A** on to the three directions. In the case of spherical polar coordinates, the natural components are those given by (8).

Tensor components may be treated in a similar way.

https://doi.org/10.1017/9781108769914.017 Published online by Cambridge University Press

The boundary conditions (5) now are

$$\left.\begin{aligned} E_\theta^{(\mathrm{I})} &= E_\theta^{(\mathrm{II})}, \quad & E_\phi^{(\mathrm{I})} &= E_\phi^{(\mathrm{II})}, \\ H_\theta^{(\mathrm{I})} &= H_\theta^{(\mathrm{II})}, \quad & H_\phi^{(\mathrm{I})} &= H_\phi^{(\mathrm{II})}. \end{aligned}\right\} \text{ for } r = a. \tag{11}$$

Eqs. (10), together with the boundary conditions (11) are the basic equations of our problem.

We shall represent the solution of these equations as a superposition of two linearly independent fields (${}^e\mathbf{E}$, ${}^e\mathbf{H}$) and (${}^m\mathbf{E}$, ${}^m\mathbf{H}$) each satisfying (10) such that

$${}^eE_r = E_r, \qquad {}^eH_r = 0, \tag{12a}$$

and

$${}^mE_r = 0, \qquad {}^mH_r = H_r. \tag{12b}$$

It is not difficult to see that such a representation is consistent with our equations. With $H_r = {}^eH_r = 0$, (10a, β) and (10a, γ) become

$$\left.\begin{aligned} k_1 {}^eE_\theta &= \frac{1}{r}\frac{\partial}{\partial r}(r {}^eH_\phi), \\ k_1 {}^eE_\phi &= -\frac{1}{r}\frac{\partial}{\partial r}(r {}^eH_\theta). \end{aligned}\right\} \tag{13}$$

Substituting from these relations into (10b, β) and (10b, γ) we obtain:

and

$$\left.\begin{aligned} \left(\frac{\partial^2}{\partial r^2} + k^2\right)(r {}^eH_\theta) &= -\frac{k_1}{\sin\theta}\frac{\partial {}^eE_r}{\partial \phi} \quad \text{(b, } \beta\text{)} \\ \left(\frac{\partial^2}{\partial r^2} + k^2\right)(r {}^eH_\phi) &= +k_1\frac{\partial {}^eE_r}{\partial \theta}. \quad \text{(b, } \gamma\text{)} \end{aligned}\right\} \tag{14}$$

Eqs. (14), together with (10a, α), constitute a system of equations for ${}^eE_r$, ${}^eH_\theta$, and ${}^eH_\phi$. Not all solutions of this system represent physical fields, however; only those do which satisfy the subsidiary conditions $\operatorname{div} {}^e\mathbf{H} = 0$. We restrict ourselves to such solutions. In spherical polar coordinates, and under our assumption that ${}^eH_r = 0$, this subsidiary condition is

$$\frac{\partial}{\partial \theta}(\sin\theta\, {}^eH_\theta) + \frac{\partial}{\partial \phi}({}^eH_\phi) = 0, \tag{15}$$

and ensures that the remaining equation (10b, α) is satisfied. For (10b, α) becomes, on substitution from (13)

$$0 = \frac{1}{k_1{}^2 r^2 \sin\theta}\frac{\partial}{\partial r}\left[\frac{\partial}{\partial \theta}(r\sin\theta {}^eH_\theta) + \frac{\partial}{\partial \phi}(r {}^eH_\phi)\right],$$

and because of (15) this is identically satisfied. Strictly similar considerations apply to the complementary case with ${}^mE_r = 0$.

The solution with vanishing radial magnetic field is called *the electric wave* (or transverse magnetic wave) and that with vanishing radial electric field is called *the magnetic wave* (or transverse electric wave). We shall now show that they may each be

https://doi.org/10.1017/9781108769914.017 Published online by Cambridge University Press

derived from a scalar potential ${}^{e}\Pi$ and ${}^{m}\Pi$ respectively, which are known as *Debye's potentials*.*

It follows, first of all from (10b, α), since ${}^{e}H_r = 0$, that ${}^{e}E_\phi$ and ${}^{e}E_\theta$ may be represented in terms of a gradient of a scalar,

$$ {}^{e}E_\phi = \frac{1}{r\sin\theta}\frac{\partial U}{\partial \phi}, \qquad {}^{e}E_\theta = \frac{1}{r}\frac{\partial U}{\partial \theta}. \tag{16} $$

If now we put

$$ U = \frac{\partial (r\ {}^{e}\Pi)}{\partial r} \tag{17} $$

then we have from (16)

$$ {}^{e}E_\theta = \frac{1}{r}\frac{\partial^2 (r\ {}^{e}\Pi)}{\partial r \partial \theta}, \qquad {}^{e}E_\phi = \frac{1}{r\sin\theta}\frac{\partial^2 (r\,{}^{e}\Pi)}{\partial r \partial \phi}. \tag{18} $$

It is seen that (13) may be satisfied by

$$ \left.\begin{aligned} {}^{e}H_\phi &= k_1 \frac{\partial {}^{e}\Pi}{\partial \theta} = \frac{k_1}{r}\frac{\partial (r\,{}^{e}\Pi)}{\partial \theta}, \\ {}^{e}H_\theta &= -\frac{k_1}{\sin\theta}\frac{\partial\,{}^{e}\Pi}{\partial \phi} = -\frac{k_1}{r\sin\theta}\frac{\partial (r\,{}^{e}\Pi)}{\partial \phi}. \end{aligned}\right\} \tag{19} $$

If we substitute from (19) into (10a, α) we obtain

$$ {}^{e}E_r = -\frac{1}{r\sin\theta}\left[\frac{\partial}{\partial\theta}\left(\sin\theta\frac{\partial\,{}^{e}\Pi}{\partial\theta}\right) + \frac{1}{\sin\theta}\frac{\partial^2\,{}^{e}\Pi}{\partial\phi^2}\right]. \tag{20} $$

Substitution from (19) and (20) into (14) gives two equations, the first of which expresses the vanishing of the ϕ derivative, the second the vanishing of the θ derivative of one and the same expression. These equations may, therefore, be satisfied by equating this expression to zero, and this gives

$$ \frac{1}{r}\frac{\partial^2 (r\,{}^{e}\Pi)}{\partial r^2} + \frac{1}{r^2\sin\theta}\frac{\partial}{\partial\theta}\left(\sin\theta\frac{\partial\,{}^{e}\Pi}{\partial\theta}\right) + \frac{1}{r^2\sin^2\theta}\frac{\partial^2\,{}^{e}\Pi}{\partial\phi^2} + k^2\,{}^{e}\Pi = 0. \tag{21} $$

By means of this equation, (20) may be written as

$$ {}^{e}E_r = \frac{\partial^2 (r\,{}^{e}\Pi)}{\partial r^2} + k^2 r\,{}^{e}\Pi. \tag{22} $$

It can be verified by substituting from (18), (19), (20), (21) and (22) into (10) that we have obtained a solution of our set of equations.

In a similar way one may consider the magnetic wave and one finds that this wave can be derived from a potential ${}^{m}\Pi$ which satisfies the same differential equation (21)

* If $\mathbf{r}$ denotes the radius vector from the origin, then ${}^{e}\Pi\mathbf{r}$ and ${}^{m}\Pi\mathbf{r}$ are *radial Hertz vectors*, i.e. Hertz vectors (see §2.2.2) which point everywhere in the radial direction. (See A. Sommerfeld, contribution in P. Frank and R. v. Mises, *Riemann-Weber's Differentialgleichungen der mathematischen Physik* (Braunschweig, Vieweg, 2nd edition, 1935; also New York, Dover Publ., 1961), Vol. 2, p. 790; C. J. Bouwkamp and H. B. G. Casimir, *Physica*, **20** (1954), 539 and A. Nisbet, *Proc. Roy. Soc.*, A, **231** (1955), 260; *Physica*, **21** (1955), 799.

https://doi.org/10.1017/9781108769914.017 Published online by Cambridge University Press

as ${}^{e}\Pi$. The complete solution of our field equations is obtained by adding the two fields; this gives

$$\left.\begin{aligned} E_r &= {}^{e}E_r + {}^{m}E_r = \frac{\partial^2(r\,{}^{e}\Pi)}{\partial r^2} + k^2 r\,{}^{e}\Pi, && (\alpha)\\ E_\theta &= {}^{e}E_\theta + {}^{m}E_\theta = \frac{1}{r}\frac{\partial^2(r\,{}^{e}\Pi)}{\partial r\partial\theta} + k_2\frac{1}{r\sin\theta}\frac{\partial(r\,{}^{m}\Pi)}{\partial\phi}, && (\beta)\\ E_\phi &= {}^{e}E_\phi + {}^{m}E_\phi = \frac{1}{r\sin\theta}\frac{\partial^2(r\,{}^{e}\Pi)}{\partial r\partial\phi} - k_2\frac{1}{r}\frac{\partial(r\,{}^{m}\Pi)}{\partial\theta}, && (\gamma) \end{aligned}\right\} \tag{23a}$$

$$\left.\begin{aligned} H_r &= {}^{m}H_r + {}^{e}H_r = k^2 r\;{}^{m}\Pi + \frac{\partial^2(r\,{}^{m}\Pi)}{\partial r^2}, && (\alpha)\\ H_\theta &= {}^{m}H_\theta + {}^{e}H_\theta = -k_1\frac{1}{r\sin\theta}\frac{\partial(r\,{}^{e}\Pi)}{\partial\phi} + \frac{1}{r}\frac{\partial^2(r\,{}^{m}\Pi)}{\partial r\partial\theta}, && (\beta)\\ H_\phi &= {}^{m}H_\phi + {}^{e}H_\phi = k_1\frac{1}{r}\frac{\partial(r\,{}^{e}\Pi)}{\partial\theta} + \frac{1}{r\sin\theta}\frac{\partial^2(r\,{}^{m}\Pi)}{\partial r\partial\phi}. && (\gamma) \end{aligned}\right\} \tag{23b}$$

Both potentials ${}^{e}\Pi$ and ${}^{m}\Pi$ are solutions of the differential equation (21), which is nothing but the wave equation

$$\nabla^2\Pi + k^2\Pi = 0,$$

written in polar coordinates. In order that the components E_θ, E_ϕ, H_θ and H_ϕ shall be continuous over the spherical surface $r = a$, it is evidently sufficient that the four quantities

$$k_1 r\,{}^{e}\Pi, \qquad k_2 r\,{}^{m}\Pi, \qquad \frac{\partial}{\partial r}(r\,{}^{e}\Pi), \qquad \frac{\partial}{\partial r}(r\,{}^{m}\Pi) \tag{24}$$

shall also be *continuous* over this surface. Thus our boundary conditions also split into independent conditions for ${}^{e}\Pi$ and ${}^{m}\Pi$. Our diffraction problem is thus reduced to the problem of finding two mutually independent solutions of the wave equation, with prescribed boundary conditions.

(b) Series expansions for the field components

We first represent the solution of the wave equations as expansions with undetermined coefficients, each term representing a particular integral. We shall then determine the coefficients by using the boundary conditions.

We seek integrals of the form

$$\Pi = R(r)\Theta(\theta)\Phi(\phi). \tag{25}$$

As may easily be verified by direct substitution into (21), the functions R, Θ and Φ must satisfy the ordinary differential equations

https://doi.org/10.1017/9781108769914.017 Published online by Cambridge University Press

$$\left.\begin{aligned} \frac{\mathrm{d}^2(rR)}{\mathrm{d}r^2} + \left(k^2 - \frac{\alpha}{r^2}\right) rR = 0, \quad &\text{(a)} \\ \frac{1}{\sin\theta}\frac{\mathrm{d}}{\mathrm{d}\theta}\left(\sin\theta\frac{\mathrm{d}\Theta}{\mathrm{d}\theta}\right) + \left(\alpha - \frac{\beta}{\sin^2\theta}\right)\Theta = 0, \quad &\text{(b)} \\ \frac{\mathrm{d}^2\Phi}{\mathrm{d}\phi^2} + \beta\Phi = 0, \quad &\text{(c)} \end{aligned}\right\} \tag{26}$$

where α and β are integration constants.

As the field **E**, **H** is a single-valued function of position, Π must likewise be single-valued, and this requirement imposes certain conditions on Θ and Φ.

For each of the equations in (26) one can write down the general solution. For (c) it is

$$a\cos(\sqrt{\beta}\phi) + b\sin(\sqrt{\beta}\phi).$$

The condition of single-valuedness demands that

$$\beta = m^2 \qquad (m = \text{integer}). \tag{27}$$

Hence the single-valued solution of (26c) is

$$\Phi = a_m\cos(m\phi) + b_m\sin(m\phi). \tag{28}$$

Eq. (26b) is the well-known equation for spherical harmonics. A necessary and sufficient condition for a single-valued solution is that

$$\alpha = l(l+1) \qquad (l > |m|, \text{ integer}). \tag{29}$$

We substitute for β from (27) in (26b) and introduce the new variable

$$\xi = \cos\theta. \tag{30}$$

The equation then transforms to*

$$\frac{\mathrm{d}}{\mathrm{d}\xi}\left[(1-\xi^2)\frac{\mathrm{d}\Theta}{\mathrm{d}\xi}\right] + \left[l(l+1) - \frac{m^2}{1-\xi^2}\right]\Theta = 0, \tag{31}$$

the solutions of which are the associated Legendre functions

$$\Theta = P_l^{(m)}(\xi) = P_l^{(m)}(\cos\theta). \tag{32}$$

These functions vanish identically if $|m| > l$; for each l there are therefore $2l+1$ such functions, namely those with

$$m = -l,\ -l+1,\ \ldots,\ l-1,\ l.$$

To integrate the remaining equation (26a) we set

$$kr = \rho, \qquad R(r) = \frac{1}{\sqrt{\rho}}Z(\rho), \tag{33}$$

and obtain the Bessel equation†

* See A. Sommerfeld, *Partial Differential Equations of Physics* (New York, Academic Press, 1949), p. 127.
† Cf. A. Sommerfeld; *loc. cit.*, p. 86.

https://doi.org/10.1017/9781108769914.017 Published online by Cambridge University Press

$$\frac{\mathrm{d}^2 Z}{\mathrm{d}\rho^2} + \frac{1}{\rho}\frac{\mathrm{d}Z}{\mathrm{d}\rho} + \left[1 - \frac{(l+\frac{1}{2})^2}{\rho^2}\right] Z = 0. \tag{34}$$

The solution of this equation is the general cylindrical function $Z = Z_{l+\frac{1}{2}}(\rho)$ of order $l+\frac{1}{2}$, so that the solution of (26a) is

$$R = \frac{1}{\sqrt{kr}} Z_{l+\frac{1}{2}}(kr). \tag{35}$$

Each cylindrical function may be expressed as a linear combination of two cylindrical functions of standard type, e.g. the Bessel functions $J_{l+\frac{1}{2}}(\rho)$ and the Neumann functions $N_{l+\frac{1}{2}}(\rho)$. For the present purpose it is convenient to employ the functions*

$$\psi_l(\rho) = \sqrt{\frac{\pi\rho}{2}} J_{l+\frac{1}{2}}(\rho), \qquad \chi_l(\rho) = -\sqrt{\frac{\pi\rho}{2}} N_{l+\frac{1}{2}}(\rho). \tag{36}$$

The functions $\psi_l(\rho)$ are regular in every finite domain of the ρ-plane, including the origin, whereas the functions $\chi_l(\rho)$ have singularities at the origin $\rho = 0$, where they become infinite. We may, therefore, use the functions $\psi_l(\rho)$ but not the functions $\chi_l(\rho)$ for representing the wave inside the sphere.

The general integral of (26a) may then be written as

$$rR = c_l \psi_l(kr) + d_l \chi_l(kr). \tag{37}$$

In particular, with $c_l = 1$, $d_l = -\mathrm{i}$ we have

$$rR = \zeta_l^{(1)}(kr), \tag{38}$$

where

$$\zeta_l^{(1)}(\rho) = \psi_l(\rho) - \mathrm{i}\chi_l(\rho) = \sqrt{\frac{\pi\rho}{2}} H^{(1)}_{l+\frac{1}{2}}(\rho), \tag{39}$$

$H^{(1)}$ being one of the Hankel functions.† The Hankel functions are distinguished from other cylindrical functions by the property that they vanish at infinity in the complex plane. The one used here with the index 1 vanishes in the half-plane of the positive imaginary part of ρ and is thus suitable for the representation of the scattered wave.

According to (25) a particular integral $\Pi_l^{(m)}$ is obtained on multiplying together the

* Several slightly different definitions of the ψ and χ functions exist in the literature. (See G. N. Watson, *A Treatise on the Theory of Bessel Functions* (Cambridge, Cambridge University Press, 2nd edition, 1944), p. 56; or A. Sommerfeld, *loc. cit.*, pp. 113–114.) On pp. 773–774 we summarize some of the formulae relating to the ψ_l functions.

† This formula is an immediate consequence of the well-known relation between the Bessel, Neumann and Hankel functions:

$$J_p + \mathrm{i}N_p = H_p^{(1)}.$$

There is a similar relation involving the other Hankel function:

$$J_p - \mathrm{i}N_p = H_p^{(2)}.$$

These two formulae are analogous to the expressions for the exponential functions $\mathrm{e}^{\mathrm{i}\rho}$ and $\mathrm{e}^{-\mathrm{i}\rho}$ in terms of $\cos\rho$ and $\sin\rho$.

https://doi.org/10.1017/9781108769914.017 Published online by Cambridge University Press

functions given by (28), (32) and (37); we then obtain the following general solution of the wave equation:

$$r\Pi = r\sum_{l=0}^{\infty}\sum_{m=-l}^{l}\Pi_l^{(m)}$$

$$= \sum_{l=0}^{\infty}\sum_{m=-l}^{l}[c_l\psi_l(kr) + d_l\chi_l(kr)][P_l^{(m)}(\cos\theta)][a_m\cos(m\phi) + b_m\sin(m\phi)], \qquad (40)$$

where a_m, b_m, c_l, and d_l are arbitrary constants.

We must now determine these constants in such a way as to satisfy the boundary conditions. For this to be possible one must be able to express the potentials ${}^e\Pi^{(i)}$ and ${}^m\Pi^{(i)}$ of the incident wave in a series of the form (40). To show that this can be done, we first transform the expression (4) for the incident wave into spherical polar coordinates in accordance with (8):

$$\left.\begin{aligned} E_r^{(i)} &= \mathrm{e}^{\mathrm{i}k^{(\mathrm{I})}r\cos\theta}\sin\theta\cos\phi, & H_r^{(i)} &= \frac{\mathrm{i}k^{(\mathrm{I})}}{k_2^{(\mathrm{I})}}\mathrm{e}^{\mathrm{i}k^{(\mathrm{I})}r\cos\theta}\sin\theta\sin\phi,\\ E_\theta^{(i)} &= \mathrm{e}^{\mathrm{i}k^{(\mathrm{I})}r\cos\theta}\cos\theta\cos\phi, & H_\theta^{(i)} &= \frac{\mathrm{i}k^{(\mathrm{I})}}{k_2^{(\mathrm{I})}}\mathrm{e}^{\mathrm{i}k^{(\mathrm{I})}r\cos\theta}\cos\theta\sin\phi,\\ E_\phi^{(i)} &= -\mathrm{e}^{\mathrm{i}k^{(\mathrm{I})}r\cos\theta}\sin\phi, & H_\phi^{(i)} &= \frac{\mathrm{i}k^{(\mathrm{I})}}{k_2^{(\mathrm{I})}}\mathrm{e}^{\mathrm{i}k^{(\mathrm{I})}r\cos\theta}\cos\phi. \end{aligned}\right\} \qquad (41)$$

To determine the potentials ${}^e\Pi^{(i)}$ or ${}^m\Pi^{(i)}$ it is only necessary to use one of (23); the first of them yields:

$$\mathrm{e}^{\mathrm{i}k^{(\mathrm{I})}r\cos\theta}\sin\theta\cos\phi = \frac{\partial^2(r\,{}^e\Pi^{(i)})}{\partial r^2} + k^{(\mathrm{I})2}r\,{}^e\Pi^{(i)}. \qquad (42)$$

The first factor on the left-hand side of this equation may be expressed in the following differentiable series of Legendre polynomials [Bauer's formula, §9.4 (9)]:

$$\mathrm{e}^{\mathrm{i}k^{(\mathrm{I})}r\cos\theta} = \sum_{l=0}^{\infty}\mathrm{i}^l(2l+1)\frac{\psi_l(k^{(\mathrm{I})}r)}{k^{(\mathrm{I})}r}P_l(\cos\theta). \qquad (43)$$

We also have the identities

$$\mathrm{e}^{\mathrm{i}k^{(\mathrm{I})}r\cos\theta}\sin\theta \equiv -\frac{1}{\mathrm{i}k^{(\mathrm{I})}r}\frac{\partial}{\partial\theta}(\mathrm{e}^{\mathrm{i}k^{(\mathrm{I})}r\cos\theta}), \qquad (44)$$

$$\frac{\partial}{\partial\theta}P_l(\cos\theta) \equiv -P_l^{(1)}(\cos\theta); \qquad P_0^{(1)}(\cos\theta) \equiv 0. \qquad (45)$$

Using these relations, the left-hand side of (42) may be expressed in the form

$$\mathrm{e}^{\mathrm{i}k^{(\mathrm{I})}r\cos\theta}\sin\theta\cos\phi = \frac{1}{(k^{(\mathrm{I})}r)^2}\sum_{l=1}^{\infty}\mathrm{i}^{l-1}(2l+1)\psi_l(k^{(\mathrm{I})}r)P_l^{(1)}(\cos\theta)\cos\phi. \qquad (46)$$

Accordingly we take as a trial solution of (42) a series of a similar form

$$r\,{}^e\Pi^{(i)} = \frac{1}{k^{(\mathrm{I})2}}\sum_{l=1}^{\infty}\alpha_l\psi_l(k^{(\mathrm{I})}r)P_l^{(1)}(\cos\theta)\cos\phi. \qquad (47)$$

https://doi.org/10.1017/9781108769914.017 Published online by Cambridge University Press

On substituting from (46) and (47) in (42) and comparing coefficients we obtain the relation

$$\alpha_l\left[k^{(\mathrm{I})2}\psi_l(k^{(\mathrm{I})}r)+\frac{\partial^2\psi_l(k^{(\mathrm{I})}r)}{\partial r^2}\right]=\mathrm{i}^{l-1}(2l+1)\frac{\psi_l(k^{(\mathrm{I})}r)}{r^2}. \tag{48}$$

Now from (37) (with $c_l=1$ and $d_l=0$) it follows that

$$\psi_l(k^{(\mathrm{I})}r)=rR \tag{49}$$

is a solution of (26a):

$$\frac{\mathrm{d}^2\psi_l}{\mathrm{d}r^2}+\left(k^{(\mathrm{I})2}-\frac{\alpha}{r^2}\right)\psi_l=0, \tag{50}$$

provided [see (29)] that $\alpha=l(l+1)$. Comparing (50) with (48), we see that

$$\alpha_l=\mathrm{i}^{l-1}\frac{2l+1}{l(l+1)}. \tag{51}$$

The calculations relating to the magnetic potential ${}^m\Pi^{(i)}$ are similar. We thus obtain the following expression for the two potentials of the incident wave:

$$\left.\begin{aligned} r\,{}^e\Pi^{(i)}&=\frac{1}{k^{(\mathrm{I})2}}\sum_{l=1}^{\infty}\mathrm{i}^{l-1}\frac{2l+1}{l(l+1)}\psi_l(k^{(\mathrm{I})}r)P_l^{(1)}(\cos\theta)\cos\phi, &&\text{(a)}\\ r\,{}^m\Pi^{(i)}&=\frac{1}{k^{(\mathrm{I})2}}\sum_{l=1}^{\infty}\mathrm{i}^{l}\frac{k^{(\mathrm{I})}}{k_2{}^{(\mathrm{I})}}\frac{2l+1}{l(l+1)}\psi_l(k^{(\mathrm{I})}r)P_l^{(1)}(\cos\theta)\sin\phi. &&\text{(b)}\end{aligned}\right\} \tag{52}$$

We have expressed both the potentials in series of the form (40) and the unknown constants can now easily be determined.

The boundary conditions (24) written more fully are

$$\left.\begin{aligned} \frac{\partial}{\partial r}[r({}^e\Pi^{(i)}+{}^e\Pi^{(s)})]_{r=a}&=\frac{\partial}{\partial r}[r\,{}^e\Pi^{(w)}]_{r=a}, &&\text{(a)}\\ \frac{\partial}{\partial r}[r({}^m\Pi^{(i)}+{}^m\Pi^{(s)})]_{r=a}&=\frac{\partial}{\partial r}[r\,{}^m\Pi^{(w)}]_{r=a}, &&\text{(b)}\\ k_1{}^{(\mathrm{I})}[r({}^e\Pi^{(i)}+{}^e\Pi^{(s)})]_{r=a}&=k_1{}^{(\mathrm{II})}[r\,{}^e\Pi^{(w)}]_{r=a}, &&\text{(c)}\\ k_2{}^{(\mathrm{I})}[r({}^m\Pi^{(i)}+{}^m\Pi^{(s)})]_{r=a}&=k_2{}^{(\mathrm{II})}[r\,{}^m\Pi^{(w)}]_{r=a}. &&\text{(d)}\end{aligned}\right\} \tag{53}$$

According to (52), these equations can only be satisfied if only those terms occur in the expansions (40) for the unknown potentials $\Pi^{(s)}$ and $\Pi^{(w)}$ for which $m=1$ and if, moreover

$$a_1=0$$

for the magnetic potential, and

$$b_1=0$$

for the electric one.

We already noted that for the representation of $\Pi^{(w)}$ only the ψ_l functions are appropriate, since these remain regular at the origin, whilst the functions χ_l become infinite there. Hence we set

https://doi.org/10.1017/9781108769914.017 Published online by Cambridge University Press

$$\left.\begin{aligned} r\,{}^{e}\Pi^{(w)} &= \frac{1}{k^{(\mathrm{II})2}}\sum_{l=1}^{\infty} {}^{e}A_l\psi_l(k^{(\mathrm{II})}r)P_l^{(1)}(\cos\theta)\cos\phi, \qquad \text{(a)}\\ r\,{}^{m}\Pi^{(w)} &= \frac{\mathrm{i}}{k^{(\mathrm{II})}k_2^{(\mathrm{II})}}\sum_{l=1}^{\infty} {}^{m}A_l\psi_l(k^{(\mathrm{II})}r)P_l^{(1)}(\cos\theta)\sin\phi. \qquad \text{(b)} \end{aligned}\right\} \tag{54}$$

We have also seen that for the scattered wave a representation in terms of the functions $\zeta_1^{(1)} = \psi_l - \mathrm{i}\chi_l$ is appropriate, $\zeta_1^{(1)}$ being obtained from the Hankel function $H^{(1)}$ on multiplication by $\sqrt{\pi\rho/2}$ [see (39)]. For large ρ, $H^{(1)}$ behaves as $\mathrm{e}^{\mathrm{i}\rho}/\sqrt{\rho}$, i.e. $\zeta_1^{(1)}$ behaves as $\mathrm{e}^{\mathrm{i}\rho}$ and $R = \zeta_1^{(1)}(k^{(\mathrm{I})}r)/r$ as $\mathrm{e}^{\mathrm{i}k^{(\mathrm{I})}r}/r$. Thus at large distances from the sphere the scattered wave is spherical, with its centre at the origin $r = 0$. We therefore set

$$\left.\begin{aligned} r\,{}^{e}\Pi^{(s)} &= \frac{1}{k^{(\mathrm{I})2}}\sum_{l=1}^{\infty} {}^{e}B_l\zeta_1^{(1)}(k^{(\mathrm{I})}r)P_l^{(1)}(\cos\theta)\cos\phi, \qquad \text{(a)}\\ r\,{}^{m}\Pi^{(s)} &= \frac{\mathrm{i}}{k^{(\mathrm{I})}k_2^{(\mathrm{I})}}\sum_{l=1}^{\infty} {}^{m}B_l\zeta_1^{(1)}(k^{(\mathrm{I})}r)P_l^{(1)}(\cos\theta)\sin\phi. \qquad \text{(b)} \end{aligned}\right\} \tag{55}$$

If we now substitute the expressions (52), (54) and (55) into the boundary conditions (53) we obtain the following linear relations between the coefficients* ${}^{e}A_l$, ${}^{m}A_l$, ${}^{e}B_l$ and ${}^{m}B_l$:

$$\left.\begin{aligned} {}^{e}B_l\frac{1}{k^{(\mathrm{I})}}\zeta_1^{(1)'}(k^{(\mathrm{I})}a) + \frac{1}{k^{(\mathrm{I})}}\mathrm{i}^{l-1}\frac{2l+1}{l(l+1)}\psi_l'(k^{(\mathrm{I})}a) &= \frac{1}{k^{(\mathrm{II})}}{}^{e}A_l\psi_l'(k^{(\mathrm{II})}a),\\ {}^{m}B_l\frac{1}{k_2^{(\mathrm{I})}}\zeta_1^{(1)'}(k^{(\mathrm{I})}a) + \frac{1}{k_2^{(\mathrm{I})}}\mathrm{i}^{l-1}\frac{2l+1}{l(l+1)}\psi_l'(k^{(\mathrm{I})}a) &= \frac{1}{k_2^{(\mathrm{II})}}{}^{m}A_l\psi_l'(k^{(\mathrm{II})}a),\\ {}^{e}B_l\frac{1}{k_2^{(\mathrm{I})}}\zeta_1^{(1)}(k^{(\mathrm{I})}a) + \frac{1}{k_2^{(\mathrm{I})}}\mathrm{i}^{l-1}\frac{2l+1}{l(l+1)}\psi_l(k^{(\mathrm{I})}a) &= \frac{1}{k_2^{(\mathrm{II})}}{}^{e}A_l\psi_l(k^{(\mathrm{II})}a),\\ {}^{m}B_l\frac{1}{k^{(\mathrm{I})}}\zeta_1^{(1)}(k^{(\mathrm{I})}a) + \frac{1}{k^{(\mathrm{I})}}\mathrm{i}^{l-1}\frac{2l+1}{l(l+1)}\psi_l(k^{(\mathrm{I})}a) &= \frac{1}{k^{(\mathrm{II})}}{}^{m}A_l\psi_l(k^{(\mathrm{II})}a). \end{aligned}\right\} \tag{56}$$

We are only interested in the coefficients ${}^{e}B_l$ and ${}^{m}B_l$ which characterize the scattered wave. These may be obtained by the elimination of ${}^{e}A_l$ and ${}^{m}A_l$; this gives

$$\left.\begin{aligned} {}^{e}B_l &= \mathrm{i}^{l+1}\frac{2l+1}{l(l+1)}\frac{k_2^{(\mathrm{I})}k^{(\mathrm{II})}\psi_l'(k^{(\mathrm{I})}a)\psi_l(k^{(\mathrm{II})}a) - k_2^{(\mathrm{II})}k^{(\mathrm{I})}\psi_l'(k^{(\mathrm{II})}a)\psi_l(k^{(\mathrm{I})}a)}{k_2^{(\mathrm{I})}k^{(\mathrm{II})}\zeta_1^{(1)'}(k^{(\mathrm{I})}a)\psi_l(k^{(\mathrm{II})}a) - k_2^{(\mathrm{II})}k^{(\mathrm{I})}\psi_l'(k^{(\mathrm{II})}a)\zeta_1^{(1)}(k^{(\mathrm{I})}a)}, \quad \text{(a)}\\ {}^{m}B_l &= \mathrm{i}^{l+1}\frac{2l+1}{l(l+1)}\frac{k_2^{(\mathrm{I})}k^{(\mathrm{II})}\psi_l(k^{(\mathrm{I})}a)\psi_l'(k^{(\mathrm{II})}a) - k_2^{(\mathrm{II})}k^{(\mathrm{I})}\psi_l'(k^{(\mathrm{I})}a)\psi_l(k^{(\mathrm{II})}a)}{k_2^{(\mathrm{I})}k^{(\mathrm{II})}\zeta_1^{(1)}(k^{(\mathrm{I})}a)\psi_l'(k^{(\mathrm{II})}a) - k_2^{(\mathrm{II})}k^{(\mathrm{I})}\zeta_l^{(1)'}(k^{(\mathrm{I})}a)\psi_l(k^{(\mathrm{II})}a)}. \quad \text{(b)} \end{aligned}\right\} \tag{57}$$

Finally, the components of the field vectors of the scattered wave are obtained on substituting from (55) in (23). This gives

* The addition of a prime to the functions ψ_l, ζ_l and $P_l^{(1)}$ denotes differentiation with respect to their arguments.

https://doi.org/10.1017/9781108769914.017 Published online by Cambridge University Press

$$
\left.
\begin{aligned}
E_r^{(s)} &= \frac{1}{k^{(\mathrm{I})2}} \frac{\cos\phi}{r^2} \sum_{l=1}^{\infty} l(l+1)\, {}^{e}B_l \zeta_l^{(1)}(k^{(\mathrm{I})} r) P_l^{(1)}(\cos\theta), \\
E_\theta^{(s)} &= -\frac{1}{k^{(\mathrm{I})}} \frac{\cos\phi}{r} \sum_{l=1}^{\infty} \left[{}^{e}B_l \zeta_l^{(1)\prime}(k^{(\mathrm{I})} r) P_l^{(1)\prime}(\cos\theta) \sin\theta \right. \\
&\qquad \left. - \mathrm{i}\, {}^{m}B_l \zeta_l^{(1)}(k^{(\mathrm{I})} r) P_l^{(1)}(\cos\theta) \frac{1}{\sin\theta} \right], \\
E_\phi^{(s)} &= -\frac{1}{k^{(\mathrm{I})}} \frac{\sin\phi}{r} \sum_{l=1}^{\infty} \left[{}^{e}B_l \zeta_l^{(1)\prime}(k^{(\mathrm{I})} r) P_l^{(1)}(\cos\theta) \frac{1}{\sin\theta} \right. \\
&\qquad \left. - \mathrm{i}\, {}^{m}B_l \zeta_l^{(1)}(k^{(\mathrm{I})} r) P_l^{(1)\prime}(\cos\theta) \sin\theta \right], \\
H_r^{(s)} &= \frac{\mathrm{i}}{k^{(\mathrm{I})} k_2^{(\mathrm{I})}} \frac{\sin\phi}{r^2} \sum_{l=1}^{\infty} l(l+1)\, {}^{m}B_l \zeta_l^{(1)}(k^{(\mathrm{I})} r) P_l^{(1)}(\cos\theta), \\
H_\theta^{(s)} &= -\frac{1}{k_2^{(\mathrm{I})}} \frac{\sin\phi}{r} \sum_{l=1}^{\infty} \left[{}^{e}B_l \zeta_l^{(1)}(k^{(\mathrm{I})} r) P_l^{(1)}(\cos\theta) \frac{1}{\sin\theta} \right. \\
&\qquad \left. + \mathrm{i}\, {}^{m}B_l \zeta_l^{(1)\prime}(k^{(\mathrm{I})} r) P_l^{(1)\prime}(\cos\theta) \sin\theta \right], \\
H_\phi^{(s)} &= \frac{1}{k_2^{(\mathrm{I})}} \frac{\cos\phi}{r} \sum_{l=1}^{\infty} \left[{}^{e}B_l \zeta_l^{(1)}(k^{(\mathrm{I})} r) P_l^{(1)\prime}(\cos\theta) \sin\theta \right. \\
&\qquad \left. + \mathrm{i}\, {}^{m}B_l \zeta_l^{(1)\prime}(k^{(\mathrm{I})} r) P_l^{(1)}(\cos\theta) \frac{1}{\sin\theta} \right].
\end{aligned}
\right\} \tag{58}
$$

This completes the formal solution of our boundary value problem. We shall not enter into the questions of existence and convergence of the solution.

It will be helpful to recall the meaning of the various constants. Since the medium surrounding the sphere is assumed to be a nonconductor, $\sigma^{(\mathrm{I})} = 0$. If we write σ in place of $\sigma^{(\mathrm{II})}$ for the conductivity of the sphere, we have from (2)

$$
\left.
\begin{aligned}
k_1^{(\mathrm{I})} &= \frac{\mathrm{i}\omega}{c} \varepsilon^{(\mathrm{I})} = \mathrm{i} \frac{2\pi}{\lambda_0} \varepsilon^{(\mathrm{I})}, \qquad k_2^{(\mathrm{I})} = \frac{\mathrm{i}\omega}{c} = \mathrm{i} \frac{2\pi}{\lambda_0}, && \text{(a)} \\
k^{(\mathrm{I})} &= \sqrt{-k_1^{(\mathrm{I})} k_2^{(\mathrm{I})}} = \frac{2\pi}{\lambda_0} \sqrt{\varepsilon^{(\mathrm{I})}} = \frac{2\pi}{\lambda^{(\mathrm{I})}}, && \text{(b)} \\
k_1^{(\mathrm{II})} &= \frac{\mathrm{i}\omega}{c} \left(\varepsilon^{(\mathrm{II})} + \mathrm{i} \frac{4\pi\sigma}{\omega} \right) = \mathrm{i} \frac{2\pi}{\lambda_0} \left(\varepsilon^{(\mathrm{II})} + \mathrm{i} \frac{4\pi\sigma}{\omega} \right), \quad k_2^{(\mathrm{II})} = \frac{\mathrm{i}\omega}{c} = \mathrm{i} \frac{2\pi}{\lambda_0}, && \text{(c)} \\
k^{(\mathrm{II})} &= \sqrt{-k_1^{(\mathrm{II})} k_2^{(\mathrm{II})}} = \frac{2\pi}{\lambda_0} \sqrt{\varepsilon^{(\mathrm{II})} + \frac{4\pi\sigma}{\omega}}, && \text{(d)}
\end{aligned}
\right\} \tag{59}
$$

where λ_0 is the wavelength of the light in the vacuum and $\lambda^{(\mathrm{I})}$ is the wavelength in the medium surrounding the sphere.

For the purpose of later discussion it is also convenient to introduce the complex refractive index of the sphere relative to the surrounding medium. Denoting this index by $\hat{n}$ we have

https://doi.org/10.1017/9781108769914.017 Published online by Cambridge University Press

$$\hat{n}^2 = \frac{\hat{n}^{(\mathrm{II})2}}{n^{(\mathrm{I})2}} = \frac{k^{(\mathrm{II})2}}{k^{(\mathrm{I})2}} = \frac{\varepsilon^{(\mathrm{II})}}{\varepsilon^{(\mathrm{I})}} + \mathrm{i}\frac{4\pi\sigma}{\omega\varepsilon^{(\mathrm{I})}} = \frac{k_1^{(\mathrm{II})}}{k_1^{(\mathrm{I})}}. \tag{60}$$

We also introduce a dimensionless parameter q defined as

$$q = \frac{2\pi}{\lambda^{(\mathrm{I})}} a, \tag{61}$$

i.e. q is 2π times the ratio of the radius of the sphere to the wavelength of the light in the outer medium. Then, using also the relation

$$\frac{k^{(\mathrm{II})} k_2^{(\mathrm{I})}}{k^{(\mathrm{I})} k_2^{(\mathrm{II})}} = \hat{n},$$

we may express the coefficients (57) in the form

$$\left.\begin{aligned} {}^{e}B_l &= \mathrm{i}^{l+1}\frac{2l+1}{l(l+1)}\frac{\hat{n}\psi_l'(q)\psi_l(\hat{n}q) - \psi_l(q)\psi_l'(\hat{n}q)}{\hat{n}\xi_l^{(1)\prime}(q)\psi_l(\hat{n}q) - \xi_l^{(1)}(q)\psi_l'(\hat{n}q)}, \quad \text{(a)} \\ {}^{m}B_l &= \mathrm{i}^{l+1}\frac{2l+1}{l(l+1)}\frac{\hat{n}\psi_l(q)\psi_l'(\hat{n}q) - \psi_l'(q)\psi_l(\hat{n}q)}{\hat{n}\xi_l^{(1)}(q)\psi_l'(\hat{n}q) - \xi_l^{(1)\prime}(q)\psi_l(\hat{n}q)}. \quad \text{(b)} \end{aligned}\right\} \tag{62}$$

These formulae take a particularly simple form when either the dielectric constant or the conductivity of the sphere is high, and at the same time the radius of the sphere is not too small. In this case $|\hat{n}| \gg 1$, $|\hat{n}q| \gg 1$ and (62) reduce to

$$\left.\begin{aligned} {}^{e}B_l &= \mathrm{i}^{l+1}\frac{2l+1}{l(l+1)}\frac{\psi_l'(q)}{\xi_l^{(1)\prime}(q)}, \quad \text{(a)} \\ {}^{m}B_l &= \mathrm{i}^{l+1}\frac{2l+1}{l(l+1)}\frac{\psi_l(q)}{\xi_l^{(1)}(q)}. \quad \text{(b)} \end{aligned}\right\} \tag{63}$$

This approximation is of little interest for optics, but it is of importance in connection with radio waves. It is also of historical interest as the early theories were concerned with this limiting case.*

(c) Summary of formulae relating to the associated Legendre functions and to the cylindrical functions

For convenience of further discussion we summarize here some formulae relating to the spherical harmonics and to the cylindrical functions.

Associated Legendre functions

The Legendre polynomials are the polynomials (in $\cos\theta$)

$$P_l(\cos\theta) = \sum_{m=0}^{[l/2]} (-1)^m \frac{(2l-2m)!}{2^l m!(l-m)!(l-2m)!}(\cos\theta)^{l-2m}, \tag{64}$$

* See K. Schwarzschild, *Münch. Akad., Math-phys. Kl.*, **31** (1901), 293.

† A slightly different definition is sometimes used, differing from the present one by a multiplicative factor $(-1)^m$.

https://doi.org/10.1017/9781108769914.017 Published online by Cambridge University Press

and the associated Legendre functions of the first kind are defined by the formula†

$$P_l^{(m)}(\cos\theta) = (\sin\theta)^m \frac{\mathrm{d}^m P_l(\cos\theta)}{\mathrm{d}(\cos\theta)^m}. \tag{65}$$

We shall also need the relations

$$\left.\begin{aligned} P_l^{(1)}(\cos\theta) &= \frac{l}{\sin\theta}[P_{l-1}(\cos\theta) - \cos\theta P_l(\cos\theta)], \\ P_l^{(1)}(\cos\theta) &= \frac{\cos\theta}{\sin^2\theta}\left[P_l{}^{(1)}(\cos\theta) - l(l+1)\frac{P_l(\cos\theta)}{\sin\theta}\right]. \end{aligned}\right\} \tag{66}$$

For large l one has the asymptotic approximation

$$P_l(\cos\theta) \sim \sqrt{\frac{2}{l\pi\sin\theta}}\sin\left[(l+\tfrac{1}{2})\theta + \frac{\pi}{4}\right]. \tag{67}$$

Cylindrical functions

I. *For small values of the argument* x, we have, for $\psi_l(x)$ the series expansion

$$\psi_l(x) = \frac{x^{l+1}}{1\times 3\times\cdots\times(2l+1)} f_l(x), \tag{68}$$

where

$$f_l(x) = 1 - \frac{2}{2l+3}\left(\frac{x}{2}\right)^2 + \cdots. \tag{69}$$

For $\zeta_l^{(1)}(x)$ we have the expansion

$$\zeta_l^{(1)}(x) = -\mathrm{i}\frac{1\times 3\times\cdots\times(2l-1)}{x^l}\mathrm{e}^{\mathrm{i}x}[h_l(x) - \mathrm{i}x g_l(x)], \tag{70}$$

where $h_l(x)$ and $g_l(x)$ are power series of which the first term is unity and the second term is quadratic in x. The functions $\psi_l'(x)$ and $\zeta_l^{(1)\prime}(x)$ may be expressed in an analogous form:

$$\psi_l'(x) = \frac{(l+1)x^l}{1\times 3\times\cdots\times(2l+1)} f_l^+(x), \tag{71}$$

$$\zeta_l^{(1)\prime}(x) = \mathrm{i}l\frac{1\times 3\times\cdots\times(2l-1)}{x^{l+1}}\mathrm{e}^{\mathrm{i}x}[h_l^+(x) - \mathrm{i}x g_l^+(x)], \tag{72}$$

where $f_l^+(x)$, $h_l^+(x)$ and $g_l^+(x)$ are power series of the same kind as before.

II. *For large values of the argument* x, provided that l is small compared with $|x|$, the following asymptotic formulae may be used:

$$\psi_l(x) \sim \tfrac{1}{2}[\mathrm{i}^{l+1}\mathrm{e}^{-\mathrm{i}x} + (-\mathrm{i})^{l+1}\mathrm{e}^{\mathrm{i}x}], \tag{73}$$

$$\zeta_l^{(1)}(x) \sim (-\mathrm{i})^{l+1}\mathrm{e}^{\mathrm{i}x}, \tag{74}$$

and

$$\psi_l'(x) \sim \tfrac{1}{2}[\mathrm{i}^{l}\mathrm{e}^{-\mathrm{i}x} + (-\mathrm{i})^{l}\mathrm{e}^{\mathrm{i}x}], \tag{75}$$

$$\zeta_l^{(1)\prime}(x) \sim (-\mathrm{i})^{l}\mathrm{e}^{\mathrm{i}x}. \tag{76}$$

https://doi.org/10.1017/9781108769914.017 Published online by Cambridge University Press

For real values of x the functions $\psi_l(x)$ and $\psi'_l(x)$ are themselves real:

$$\psi_l(x) \sim \sin\left(x - \frac{l\pi}{2}\right), \tag{77}$$

$$\psi'_l(x) \sim \cos\left(x - \frac{l\pi}{2}\right). \tag{78}$$

14.5.2 Some consequences of Mie's formulae

(a) The partial waves

It is seen from (58) that the amplitude of the radial components $E_r^{(s)}$ and $H_r^{(s)}$ of the scattered wave fall off as the inverse square of the distance from the scattering centre, whereas the amplitudes of the other components fall off more slowly, as the inverse of this distance. At sufficiently great distances ($r \gg \lambda$), in the *radiation zone* or *wave zone*, the radial components may, therefore, be neglected in comparison with the tangential components, i.e. in this region the wave is *transverse*.

The formulae show that the scattered wave is composed of contributions involving spherical harmonics of different orders. These contributions may be called *partial waves* and their strength is determined by the absolute values of the complex coefficients ${}^eB_l$ and ${}^mB_l$. These coefficients depend on the nature of the two media, and on the ratio of the radius of the sphere to the wavelength of the incident light.

Each partial wave consists of an electrical part with amplitude ${}^eB_l$ and a magnetic part with amplitude ${}^mB_l$. The magnetic lines of force of the electric partial wave and the electric lines of force of the magnetic partial wave lie wholly on concentric spherical surfaces, since for the former $H_r^{(s)} = 0$ and for the latter $E_r^{(s)} = 0$.

Let us consider a typical partial wave, for instance the lth electric wave. We see that the corresponding components $E_\theta^{(s)}$ and $H_\phi^{(s)}$ vanish at points where either $\cos\phi$ or $P_l^{(1)\prime}(\cos\theta)\sin\theta$ is zero; likewise $E_\phi^{(s)}$ and $H_\theta^{(s)}$ vanish where either $\sin\phi$ or $P_l^{(1)}(\cos\theta)/\sin\theta$ is zero. Now within the interval $0 \leqslant \theta \leqslant \pi$, the function $P_l^{(1)\prime}(\cos\theta)$ vanishes l times and the function $P_l^{(1)}(\cos\theta)/\sin\theta$ vanishes $(l-1)$ times, but differs from zero when $\theta = 0$ or π. It follows that for $\phi = \pm\pi/2$ all the field components vanish $2l$ times, i.e. $(4l-2)$ times in all. As the magnetic lines of force must be closed curves, and as we saw they lie wholly on spherical surfaces concentric with the origin, it follows that each of the $2l$ zero points on the circle $\phi = 0$ or π are the centres of families of closed magnetic loops, whereas the $2(l-1)$ zero points lying on the circle $\phi = \pm\pi/2$ are neutral points. The lines of force avoid these neutral points just as two families of rectangular hyperbolae having common asymptotes avoid their common centre.

Fig. 14.8 shows the magnetic lines of force for the fourth electrical partial wave. The two sets of points may be clearly distinguished; the first in the xz-section (the plane of the diagram) and the second in the yz-section.

Fig. 14.9(a) shows the projections on to the y, z-plane of the magnetic lines of force situated on one of the two hemispheres on either side of the y, z-plane, and belonging to the first four electric partial waves. In the radiation zone the electric lines of force are orthogonal to the magnetic lines, since, according to (58), one has, for each partial wave (electric or magnetic),

https://doi.org/10.1017/9781108769914.017 Published online by Cambridge University Press

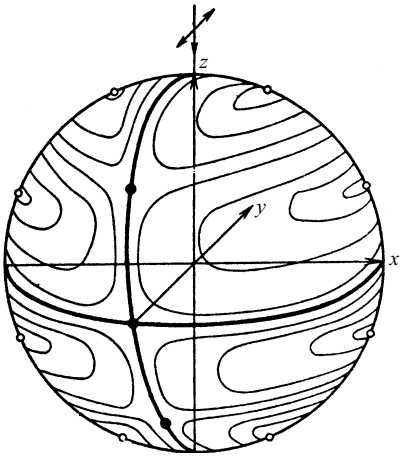

Fig. 14.8 Lines of magnetic force for the fourth electric partial wave.

$$E_\theta^{(s)} H_\theta^{(s)} + E_\phi^{(s)} H_\phi^{(s)} = 0. \tag{79}$$

Fig. 14.9(b) shows these lines in a similar projection on the x, z-plane.

Similar results hold for the magnetic partial waves, except that $\cos\phi$ and $\sin\phi$ are now interchanged. The corresponding projections of the electric lines of force of the magnetic partial waves that lie on a sphere may be obtained merely be rotating the figures through an angle of 90° about the z-axis.

(b) Limiting cases

We shall now investigate the relative contributions of the various partial waves. The general case ($\hat{n}$ and q arbitrary) is not amenable to simple analytical treatment and we, therefore, consider in detail only two limiting cases, namely when the radius of the sphere is large compared with the wavelength ($q \gg 1$), and when it is much smaller than a wavelength ($q \ll 1$).

I: $q \gg 1$. This is the case for which our solution must be expected to give substantially the same results as the Huygens–Kirchhoff diffraction theory, or even (as $q \to \infty$) the same results as geometrical optics.

If we restrict ourselves to orders l that are very much less than q and $|\hat{n}q|$ then we may use the asymptotic approximations (73)–(76). We have

$$\frac{\psi_l(\hat{n}q)}{\psi_l'(\hat{n}q)} \sim \frac{\mathrm{i}^{l+1}\mathrm{e}^{-\mathrm{i}\hat{n}q} + (-\mathrm{i})^{l+1}\mathrm{e}^{\mathrm{i}\hat{n}q}}{\mathrm{i}^{l}\mathrm{e}^{-\mathrm{i}\hat{n}q} + (-\mathrm{i})^{l}\mathrm{e}^{\mathrm{i}\hat{n}q}} = \frac{\cos\left[\hat{n}q - (l+1)\dfrac{\pi}{2}\right]}{\cos\left(\hat{n}q - l\dfrac{\pi}{2}\right)} = \tan\left(\hat{n}q - l\frac{\pi}{2}\right), \tag{80}$$

and the coefficients (62) become

https://doi.org/10.1017/9781108769914.017 Published online by Cambridge University Press

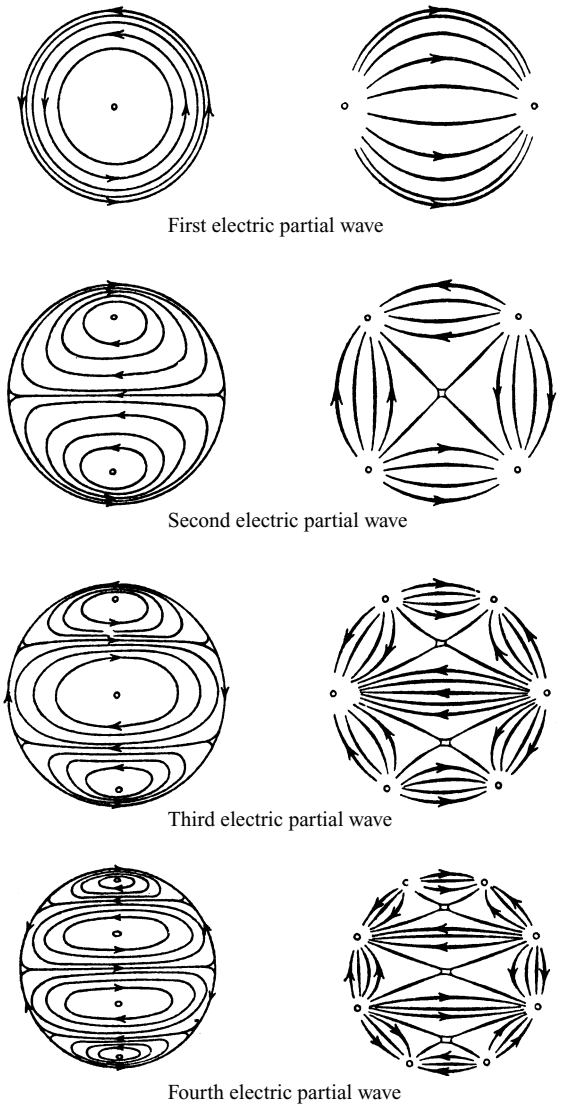

Fig. 14.9 Lines of force of the first four electric partial waves: (a) magnetic lines of force; (b) electric lines of force. [After G. Mie, *Ann. d. Physik* (4), **25** (1908), 377].

$$\left.\begin{aligned} {}^{e}B_l &= (-1)^{l+1}\frac{2l+1}{l(l+1)}\mathrm{e}^{-\mathrm{i}q}\frac{\sin\left(q-l\frac{\pi}{2}\right)-\hat{n}\cos\left(q-l\frac{\pi}{2}\right)\tan\left(\hat{n}q-l\frac{\pi}{2}\right)}{1-\mathrm{i}\hat{n}\tan\left(\hat{n}q-l\frac{\pi}{2}\right)} \\ {}^{m}B_l &= (-1)^{l+1}\frac{2l+1}{l(l+1)}\mathrm{e}^{-\mathrm{i}q}\frac{\hat{n}\sin\left(q-l\frac{\pi}{2}\right)-\cos\left(q-l\frac{\pi}{2}\right)\tan\left(\hat{n}q-l\frac{\pi}{2}\right)}{\hat{n}-\mathrm{i}\tan\left(\hat{n}q-l\frac{\pi}{2}\right)}. \end{aligned}\right\} \quad (81)$$

https://doi.org/10.1017/9781108769914.017 Published online by Cambridge University Press

We note that these coefficients are rapidly oscillating functions of both q and l, so that a small change in q or l may give rise to a large change in ${}^eB_l$ and ${}^mB_l$. We also observe that ${}^mB_{l+1}$ and ${}^eB_l$ are of the same order of magnitude, i.e. the amplitude of the electric partial wave of order l is of the same order of magnitude as that of the magnetic partial wave of next higher order.

Since the formulae (81) were derived on the assumption that l is much smaller than q, one cannot determine from these approximations the number of partial waves that make an appreciable contribution to the scattered field. Debye* derived asymptotic approximations valid for all orders and showed that the amplitudes of the partial waves fall off rapidly to zero as soon as $l+\frac{1}{2}$ exceeds q, so that only the first q terms need be included.

When either the dielectric constant or the conductivity of the sphere is very large ($|\hat{n}| \to \infty$), the expressions for ${}^eB_l$ and ${}^mB_l$ reduce to

$$\left.\begin{aligned} {}^eB_l &= \mathrm{i}(-1)^{l+1}\frac{2l+1}{l(l+1)}\mathrm{e}^{-\mathrm{i}q}\cos\left(q-l\frac{\pi}{2}\right), \\ {}^mB_l &= (-1)^{l+1}\frac{2l+1}{l(l+1)}\mathrm{e}^{-\mathrm{i}q}\sin\left(q-l\frac{\pi}{2}\right), \end{aligned}\right\} \tag{82}$$

derived most simply from (63) with the help of the asymptotic approximations (73)–(76).

The approximations of this section ($q \gg 1$) may be applied in connection with the theory of the rainbow;† the parameter q, determined by the size of the raindrops, is of the order 10^4.

II: $q \ll 1$. This case is of great practical importance in connection with microscopic and submicroscopic particles in colloidal solutions. We may now use the power series expansions (68)–(72) for the cylindrical functions and obtain (restricting ourselves to terms of the leading order),

$$\left.\begin{aligned} {}^eB_l &\sim \mathrm{i}^l\frac{q^{2l+1}}{l^2[1\times3\times5\times\cdots\times(2l-1)]^2}\frac{\hat{n}^2-1}{\hat{n}^2+\dfrac{l+1}{l}}, \\ {}^mB_l &\sim \mathrm{i}^l\frac{q^{2l+3}}{l(l+1)(2l+1)(2l+3)[1\times3\times5\times\cdots\times(2l-1)]^2}(\hat{n}^2-1). \end{aligned}\right\} \tag{83}$$

When either the conductivity or the dielectric constant is very large, we have from (63)‡

* P. Debye, *Ann. d. Physik* (4), **30** (1909), 118; *Mat. Ann.*, **67** (1909), 535; *Sitzungsb. Münch. Akad. Wiss, Math. Phys. Kl.*, 5 Abh. (1910).

† See B. van der Pol and H. Bremmer, *Phil. Mag.*, (7), **24** (1937), 857; H. Bucerius, *Optik*, **1** (1946), 188.

‡ A direct transition from (83) to (84) is not simple; one has to take into account that as $|\hat{n}| \to \infty$, $q \to 0$ in such a way that $q^2|\hat{n}|^2$ approaches a finite value.

https://doi.org/10.1017/9781108769914.017 Published online by Cambridge University Press

$$\left.\begin{aligned} {}^{e}B_l &= \mathrm{i}^l \frac{q^{2l+1}}{l^2[1\times 3\times 5\times\cdots\times(2l-1)]^2}, \\ {}^{m}B_l &= -\mathrm{i}^l \frac{q^{2l+1}}{l(l+1)[1\times 3\times 5\times\cdots\times(2l-1)]^2}. \end{aligned}\right\} \tag{84}$$

As long as the conductivity remains finite [formulae (83)], ${}^{e}B_{l+1}$ and ${}^{m}B_l$ are proportional to the same power of q, i.e. the amplitude of the $(l+1)$th electric partial wave is of the same order of magnitude as the amplitude of the lth magnetic partial wave, just as was the case when $q \gg 1$. If the radius of the sphere is so small that q^2 may be neglected in comparison with unity, only the first electric partial wave need be considered and its strength (and phase) is given by the complex amplitude

$${}^{e}B_l = \mathrm{i}q^3 \frac{\hat{n}^2-1}{\hat{n}^2+2} = \mathrm{i}\left(\frac{2\pi a}{\lambda^{(\mathrm{I})}}\right)^3 \frac{\hat{n}^2-1}{\hat{n}^2+2}. \tag{85}$$

Since ${}^{e}B_l$ is complex there is a phase difference between the incident primary field and the scattered secondary field.

On the other hand, in the limiting case $|\hat{n}| \to \infty$, the amplitude of the lth electric partial wave and the amplitude of the lth magnetic partial wave are of the same order of magnitude, as is seen from (84).

Let us now consider, for $|\hat{n}|$ finite, the field of the first electric partial wave, at large distances from the sphere ($r \gg \lambda$). We use in (58) the asymptotic approximations

$$\xi_1^{(1)}(x) = -\mathrm{e}^{\mathrm{i}x}, \qquad \xi_1^{(1)\prime}(x) = -\mathrm{i}\mathrm{e}^{\mathrm{i}x}, \tag{86}$$

and the relations

$$P_1(\cos\theta) = \cos\theta, \qquad P_1^{(1)}(\cos\theta) = \sin\theta, \qquad P_1^{(1)\prime}(\cos\theta)\sin\theta = -\cos\theta, \tag{87}$$

where the prime denotes differentiation with respect to $\cos\theta$, and obtain:

$$\left.\begin{aligned} E_\theta^{(s)} &= -\frac{\mathrm{i}}{k^{(\mathrm{I})}}\cos\phi\cos\theta\,{}^{e}B_1\frac{\mathrm{e}^{\mathrm{i}k^{(\mathrm{I})}r}}{r} = \left(\frac{2\pi}{\lambda^{(\mathrm{I})}}\right)^2 a^3\frac{\hat{n}^2-1}{\hat{n}^2+2}\cos\phi\cos\theta\frac{\mathrm{e}^{\mathrm{i}k^{(\mathrm{I})}r}}{r}, \\ E_\phi^{(s)} &= \frac{\mathrm{i}}{k^{(\mathrm{I})}}\sin\phi\,{}^{e}B_1\frac{\mathrm{e}^{\mathrm{i}k^{(\mathrm{I})}r}}{r} = -\left(\frac{2\pi}{\lambda^{(\mathrm{I})}}\right)^2 a^3\frac{\hat{n}^2-1}{\hat{n}^2+2}\sin\phi\,\frac{\mathrm{e}^{\mathrm{i}k^{(\mathrm{I})}r}}{r}, \\ H_\theta^{(s)} &= \frac{1}{k_2^{(\mathrm{I})}}\sin\phi\,{}^{e}B_1\frac{\mathrm{e}^{\mathrm{i}k^{(\mathrm{I})}r}}{r} = \left(\frac{2\pi}{\lambda^{(\mathrm{I})}}\right)^2\sqrt{\varepsilon^{(\mathrm{I})}}a^3\frac{\hat{n}^2-1}{\hat{n}^2+2}\sin\phi\,\frac{\mathrm{e}^{\mathrm{i}k^{(\mathrm{I})}r}}{r}, \\ H_\phi^{(s)} &= \frac{1}{k_2^{(\mathrm{I})}}\cos\phi\cos\theta\,{}^{e}B_1\frac{\mathrm{e}^{\mathrm{i}k^{(\mathrm{I})}r}}{r} = \left(\frac{2\pi}{\lambda^{(\mathrm{I})}}\right)^2\sqrt{\varepsilon^{(\mathrm{I})}}a^3\frac{\hat{n}^2-1}{\hat{n}^2+2}\cos\phi\cos\theta\,\frac{\mathrm{e}^{\mathrm{i}k^{(\mathrm{I})}r}}{r}. \end{aligned}\right\} \tag{88}$$

It is easy to see that equations (88) are identical with those for the radiation zone ($r \gg \lambda$) of an *electric dipole at O, oscillating parallel to the x-axis*, i.e. parallel to the electric vector of the primary incident field, and of moment $p = p_0\,\mathrm{e}^{-\mathrm{i}\omega t}$, where

$$p_0 = a^3\left|\frac{\hat{n}^2-1}{\hat{n}^2+2}\right|. \tag{89}$$

To show this we assume first that the outer medium is vacuum ($\varepsilon^{(\mathrm{I})} = 1$) and we return

https://doi.org/10.1017/9781108769914.017 Published online by Cambridge University Press

to §2.2 (53) and §2.2 (54). According to these equations, the radiation field in vacuum of a linear electric dipole of moment $\mathbf{p}_0\,\mathrm{e}^{-\mathrm{i}\omega t}$ is given by

$$\left.\begin{aligned}\mathbf{E} &= -\left(\frac{\omega}{c}\right)^2 \frac{1}{r^3}\mathbf{r}\times(\mathbf{r}\times\mathbf{p}_0),\\ \mathbf{H} &= \left(\frac{\omega}{c}\right)^2 \frac{1}{r^2}(\mathbf{r}\times\mathbf{p}_0),\end{aligned}\right\} \tag{90}$$

where the time-harmonic factor $\mathrm{e}^{-\mathrm{i}\omega t}$ has been omitted and $\mathbf{r}$ is the position vector of the point of observation with respect to the origin. From (90) it follows that if $\mathbf{p}_0$ is the direction of the x-axis, the components of $\mathbf{E}$ and $\mathbf{H}$ are given by

$$\left.\begin{aligned}E_x &= \left(\frac{\omega}{c}\right)^2 p_0(\sin^2\theta\sin^2\phi+\cos^2\theta)\frac{\mathrm{e}^{\mathrm{i}kr}}{r},\\ E_y &= -\left(\frac{\omega}{c}\right)^2 p_0(\sin^2\theta\sin\phi\cos\phi)\frac{\mathrm{e}^{\mathrm{i}kr}}{r},\\ E_z &= -\left(\frac{\omega}{c}\right)^2 p_0\sin\theta\cos\theta\cos\phi\,\frac{\mathrm{e}^{\mathrm{i}kr}}{r},\\ H_x &= 0,\\ H_y &= \left(\frac{\omega}{c}\right)^2 p_0\cos\theta\,\frac{\mathrm{e}^{\mathrm{i}kr}}{r},\\ H_z &= -\left(\frac{\omega}{c}\right)^2 p_0\sin\theta\sin\phi\,\frac{\mathrm{e}^{\mathrm{i}kr}}{r}.\end{aligned}\right\} \tag{91}$$

If now the transformation (8) to spherical polar coordinates is applied, this transforms into (88) (with $\varepsilon^{(\mathrm{I})}=1$) if the expression (89) is substituted for p_0. In the more general case, when $\varepsilon^{(\mathrm{I})}\neq 1$, we must consider in place of (91) the corresponding expressions for the radiation field of a dipole in a dielectric. These expressions, which may be obtained in a similar way to (91), transform into (88) when transformation to spherical polar coordinates is made. We note that the refractive index of the sphere enters the expression (89) for the equivalent dipole moment only in the combination $(\hat{n}^2-1)/(\hat{n}^2+2)$; for dielectric substances (n real) we have already encountered this expression, in the theory of molecular refractivity [see §2.3 (17)].

Since, according to (88) the amplitude is inversely proportional to the square of the wavelength, the intensity of the scattered light is inversely proportional to the fourth power of the wavelength. In such a case one speaks of *Rayleigh scattering*.*

The first magnetic partial wave may be similarly described in terms of a vibrating magnetic dipole. The partial waves of higher orders may be considered to be due to vibrating multipoles, but we shall not investigate this here.

* As already pointed out on p. 104, Rayleigh showed, in celebrated papers concerning the blue colour of the sky, that scattering of this type is also caused by spontaneous fluctuations in the density of a homogeneous medium. (Lord Rayleigh, *Phil. Mag.*, (4), **XLI** (1871), 274, 447; (5), **XLVII** (1899), 375. Reprinted in his *Scientific Papers by John William Strutt, Baron Rayleigh* (Cambridge, Cambridge University Press, 1899–1920), Vol. 1, pp. 87, 104; Vol. 4, p. 397.)

https://doi.org/10.1017/9781108769914.017 Published online by Cambridge University Press

(c) Intensity and polarization of the scattered light

Let us now return to the general case and examine briefly the intensity and the polarization of the scattered light. As we are only interested in relative values of the intensity we may take as a measure of the intensity the square of the real amplitude of the electric vector. We consider only the distant field ($r \gg \lambda$) and may therefore replace the functions $\zeta_l^{(1)}$ and $\zeta_l^{(1)\prime}$ in (58) by their asymptotic approximations. We also set

$$\left.\begin{aligned} I_{\parallel}^{(s)} &= \frac{\lambda^{(\mathrm{I})2}}{4\pi^2 r^2}\left|\sum_{l=1}^{\infty}(-\mathrm{i})^l\left[{}^{e}B_l P_l^{(1)\prime}(\cos\theta)\sin\theta - {}^{m}B_l\frac{P_l^{(1)}(\cos\theta)}{\sin\theta}\right]\right|^2,\\ I_{\perp}^{(s)} &= \frac{\lambda^{(\mathrm{I})2}}{4\pi^2 r^2}\left|\sum_{l=1}^{\infty}(-\mathrm{i})^l\left[{}^{e}B_l\frac{P_l^{(1)}(\cos\theta)}{\sin\theta} - {}^{m}B_l P_l^{(1)\prime}(\cos\theta)\sin\theta\right]\right|^2. \end{aligned}\right\} \tag{92}$$

Then

$$|E_\theta^{(s)}|^2 = I_{\parallel}^{(s)}\cos^2\phi, \qquad |E_\phi^{(s)}|^2 = I_{\perp}^{(s)}\sin^2\phi. \tag{93}$$

We define the *plane of observation* as the plane that contains the direction of propagation of the incident light and the direction (θ, ϕ) of observation. According to (4) and (7), ϕ represents the angle between this plane and the direction of vibration of the electric vector of the incident wave. Since according to (93) either $E_\theta^{(s)}$ or $E_\phi^{(s)}$ vanishes when $\phi = 0$ or $\phi = \pi/2$, the scattered light is linearly polarized when the plane of observation is parallel or perpendicular to the primary vibrations. For any other direction (θ, ϕ) the light is in general elliptically polarized, since the ratio $E_\theta^{(s)}/E_\phi^{(s)}$ is complex. In the special case of Rayleigh scattering, represented by (88), the ratio $E_\theta^{(s)}/E_\phi^{(s)}$ is, however, always real, so that the scattered light is then linearly polarized for all directions of observation.

In practice one is usually concerned with the scattering of *natural light*. As in §1.5 the appropriate formulae may be obtained from those for polarized light by averaging over all directions of polarization.* Denoting by a bar this average, we now have, in place of (93), since $\overline{\cos^2\phi} = \overline{\sin^2\phi} = \frac{1}{2}$,

$$\overline{|E_\theta^{(s)}|^2} = \tfrac{1}{2}I_{\parallel}{}^{(s)}, \qquad \overline{|E_\phi^{(s)}|^2} = \tfrac{1}{2}I_{\perp}. \tag{94}$$

In general neither $I_{\parallel}^{(s)}$ nor $I_{\perp}^{(s)}$ is zero, so that the scattered light is partially polarized. In analogy with §1.5 (42) we may define the degree of polarization P of the scattered light as

$$P = \left|\frac{I_{\perp}^{(s)} - I_{\parallel}^{(s)}}{I_{\perp}^{(s)} + I_{\parallel}^{(s)}}\right|. \tag{95}$$

The unpolarized portion of the scattered light then is

* Alternatively we may use the result of §10.9.2, according to which a wave of natural light may be regarded as composed of two incoherent waves of equal amplitudes, propagated in the same direction and polarized in directions at right angles to each other. The scattering of each wave may be determined separately and the total intensity is obtained by summing the intensities of the two component waves. This leads again to (94).

https://doi.org/10.1017/9781108769914.017 Published online by Cambridge University Press

$$\left.\begin{aligned}(I_{\perp}^{(s)} + I_{\parallel}^{(s)})(1-P) &= 2I_{\parallel}^{(s)} \quad \text{when} \quad I_{\parallel}^{(s)} < I_{\perp}^{(s)},\\ &= 2I_{\perp}^{(s)} \quad \text{when} \quad I_{\parallel}^{(s)} > I_{\perp}^{(s)}.\end{aligned}\right\} \tag{96}$$

The dependence of the intensity and polarization of the scattered light on the direction of scattering and on the physical parameters (λ, a, $\hat{n}$) has been investigated on the basis of Mie's theory by many writers* and we cannot do more here than summarize briefly some of the main results obtained.

In Figs. 14.10 and 14.11 the intensity and the unpolarized proportion of the scattered light are shown as functions of the angle θ of observation for dielectric and metallic spheres of various sizes. The length of the radius vector of the outer curves is proportional to the intensity $I^{(s)} = I_{\parallel}^{(s)} + I_{\perp}^{(s)}$ and that of the inner curves, unless stated otherwise, is proportional to $I_{\perp}^{(s)}$. The units are arbitrary and different in each figure. From these *polar diagrams* as well as from other published calculations the following general conclusions may be drawn:

Excluding the case when the conductivity or the dielectric constant is very large (in which case most of the incident light is radiated in the backward direction, i.e. 'reflected'), the polar diagrams, in the limit of vanishingly small spheres ($a \to 0$), are symmetrical about the plane through the centre of the sphere, at right angles to the

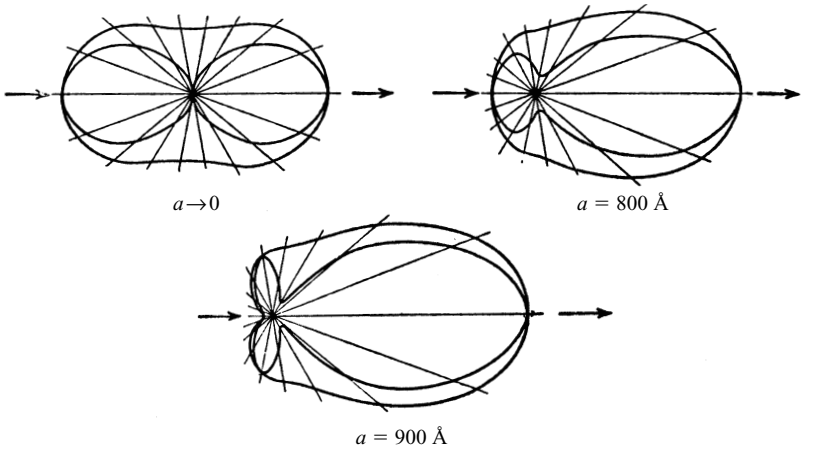

Fig. 14.10 Polar diagrams for the scattering of linearly polarized light by a spherical gold particle ($\lambda_0 = 5500$ Å, $n^{(\mathrm{I})} = 1.33$, $\hat{n}^{(\mathrm{II})} = 0.57 + 2.45\mathrm{i}$). (After G. Mie, *Ann. d. Phys.*, (4), **25** (1908), 429.)

* In addition to the paper by Mie already quoted we may refer to the following:

R. Gans, *Ann. d. Physik* (4), **76** (1925), 29; H. Senftleben and E. Benedict, *Ann. d. Physik* (4), **60** (1919), 297; H. Blumer, *Z. Phys.*, **32** (1925), 119; **38** (1926), 304, 920; **39** (1926), 195; C. Schalén, *Uppsala Astr. Obs. Ann.*, **1**, No. 2 (1939); *ibid*., **1**, No. 9 (1945); G. R. Paranjpe, Y. G. Naik and P. B. Vaidya, *Proc. Indian Acad.*, A, **9** (1939), 333, 352; H. Holl, *Optik*, **1** (1946), 213; *ibid*., **4** (1948/49), 173. A very full survey of results obtained by many writers will be found in a paper by H. C. van de Hulst, *Rech. Astr. Observ. Utrecht*, **11**, Pt. I (1946) and in his book *Light Scattering by Small Particles* (New York, John Wiley and Sons; London, Chapman and Hall, 1957). See also G. Oster, *Chem. Rev.*, **43** (1948), 319.

Tables of scattering functions for spherical particles, National Bureau of Standards (Washington, DC 1949), Applied Mathematics Series, Vol. 4; R. O. Gumprecht and C. M. Sliepcevich, *Light-Scattering Functions for Spherical Particles* (Ann Arbor, University of Michigan Press, 1951).

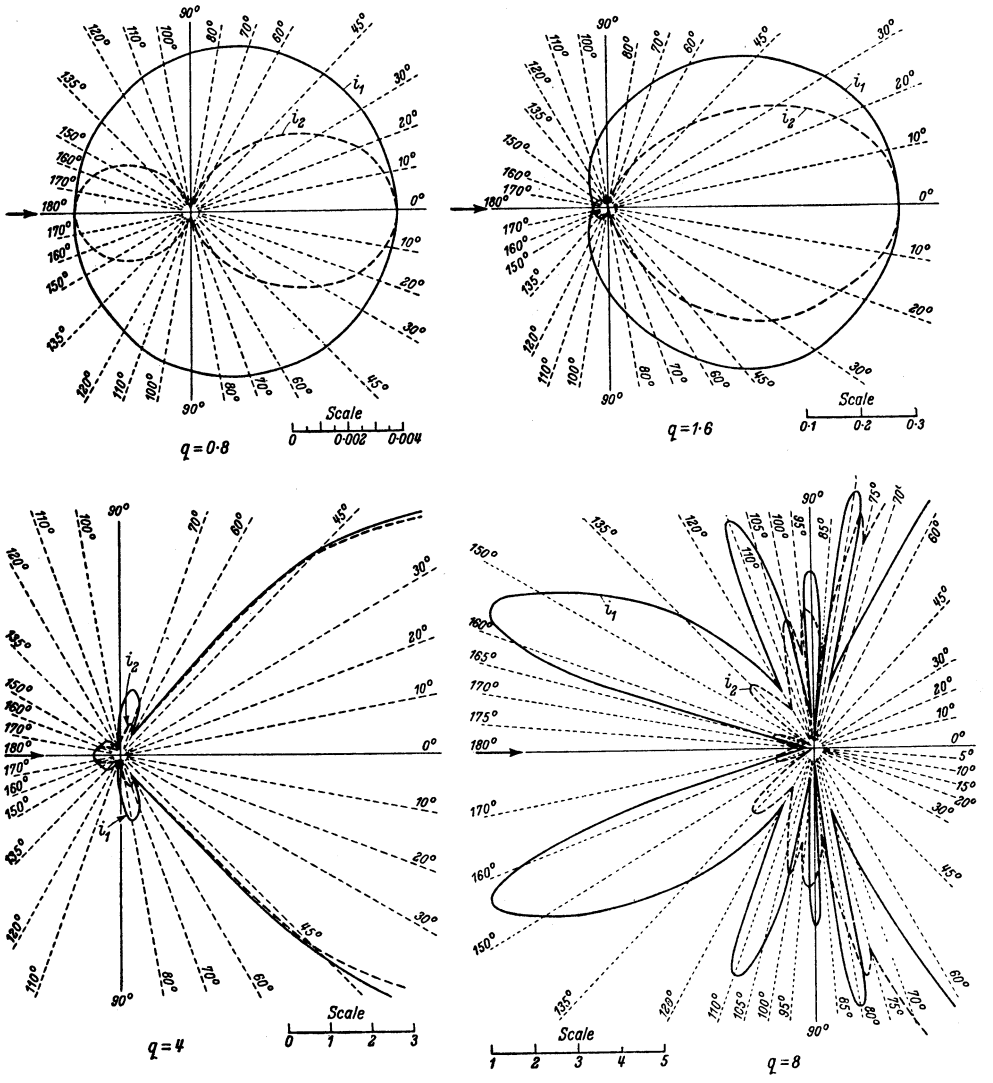

Fig. 14.11 Polar diagrams for the scattering of linearly polarized light by a dielectric sphere of refractive index $n = 1.5$: $i_1 = q^2 I_\perp$, $i_2 = q^2 I_\parallel$. (After H. Bulmer, *Z. Phys.*, **32** (1925), 119.)

direction of propagation of the incident light. There is an intensity maximum in the forward direction ($\theta = 0$) and in the reverse direction ($\theta = 180°$), and there is a minimum in the plane of symmetry ($\theta = 90°$). As the radius of the sphere is increased there is a departure from symmetry, more light being scattered in the forward direction than in the opposite direction. This phenomenon is often called the *Mie effect*. As the radius is increased still further practically all the scattered light appears around the forward direction $\theta = 0$; likewise for a conducting sphere there is a greater concentration of light in this direction. When the radius of the sphere is very large compared to the wavelength most of the incident light is, however, reflected, as follows from geometrical optics.

https://doi.org/10.1017/9781108769914.017 Published online by Cambridge University Press

Table 14.4. *The normalized intensity* $4\pi^2 a^2 (I_\perp^{(s)} + I_\parallel^{(s)})/\lambda^{(\mathrm{I})2}$ *of light scattered by dielectric spheres of refractive index* $n = 1.25$*, as function of the parameter* $q = 2\pi a/\lambda^{(\mathrm{I})}$.

θ	$q = 0.01$	$q = 0.1$	$q = 0.5$	$q = 1$	$q = 2$	$q = 5$	$q = 8$
0	5.0×10^{-14}	5.0×10^{-8}	1.2×10^{-3}	2.3×10^{-1}	4.3	9.8×10^{2}	7.5×10^{3}
90°	2.5×10^{-14}	2.5×10^{-8}	5.0×10^{-4}	3.6×10^{-2}	2.5×10^{-1}	2.7	7.1
180°	5.0×10^{-14}	4.9×10^{-8}	7.8×10^{-4}	1.9×10^{-3}	2.0×10^{-2}	1.3	0.9

(Compiled from calculations of H. Blumer, *Z. Phys.*, **38** (1926), 304.)

The dependence of the intensity of the scattered light on the radius of the sphere is illustrated in Table 14.4. The Mie effect may be clearly seen from the comparison of the first and third row. The table indicates a very rapid increase in intensity with increasing size of the sphere; for true comparison the values in the table must be multiplied by the factor $\lambda^{(\mathrm{I})2}/4\pi^2 a^2 = 1/q^2$.

When q exceeds unity, i.e. when the diameter $2a$ of the sphere is greater than $\lambda^{(\mathrm{I})}/\pi$ there appears a series of maxima and minima, which at first are distributed irregularly. The appearance of a number of maxima and minima when q is large is in agreement with the Huygens–Kirchhoff theory.

Concerning polarization of the scattered light the results again are different depending on whether or not $|\hat{n}|$ is large.

For very small spheres which are highly conducting ($\sigma \to \infty$) or have very high dielectric constant ($\varepsilon \to \infty$) the polarization is largest when $\theta = 60°$ (the Thomson angle). With increasing radius the maximum is displaced in the direction of increasing θ.

The dependence of the polarization on the angle θ of observation, for spheres of finite conductivity and finite dielectric constant, is illustrated in two typical cases in Figs. 14.10 and 14.11. When the radius of the sphere is very small ($q \to 0$), the polarization diagram is, like the intensity diagram, symmetrical about the x, y-plane and has a maximum for $\theta = 90°$, where the polarization is complete. In this case (Rayleigh scattering), the degree of polarization may be represented by a single analytical expression, obtained on substituting from (88) and (93) into (95); this gives

$$P(\theta) = \frac{\sin^2\theta}{1 + \cos^2\theta}. \tag{97}$$

This formula was derived by Rayleigh, in a different way.

As the radius of the sphere is increased, up to about $a = \lambda^{(\mathrm{I})}/\pi$, the maximum is displaced; in the majority of the cases that have been investigated the displacement is in the direction of larger θ for dielectric spheres and in the direction of smaller θ for absorbing spheres. When the radius of the sphere is increased still further, there appears an irregular sequence of polarization maxima.

In the direction $\theta = 90°$ the light is, for $q < 1$, almost completely polarized, with its electric vector perpendicular to the plane of observation; for larger values of q this is no longer the case and the behaviour becomes irregular.

So far we have confined our attention to monochromatic light. One often deals with

https://doi.org/10.1017/9781108769914.017 Published online by Cambridge University Press

scattering of polychromatic light and we must therefore also consider the effects arising from the presence of components of different wavelengths. We note that the wavelength enters our formulae only through the parameter q and through the refractive index $\hat{n}$. In a sufficiently small range of wavelengths, $\hat{n}$ is practically independent of the wavelength if in (60) the term that contains the conductivity σ is small compared with the other term, i.e. for a poorly conducting sphere. On the other hand, in the limit of infinitely high conductivity, $\hat{n}$ does not enter at all. In these cases the intensities of the spectral components depend on $a/\lambda^{(\mathrm{I})}$ only. The effect of changing the wavelength is thus substantially equivalent to the effect that arises from changing the radius of the sphere by an appropriate amount. Since for different wavelengths the polarization maxima occur at different angles of observations, complicated colour changes are seen when observations on scattered light are made through a polarizing prism. This effect is called *polychroism*. The dependence of polarization of the scattered light on wavelength – known as *dispersion of polarization* – affords a very precise test of the theory.*

14.5.3 Total scattering and extinction

(a) Some general considerations

It is of considerable practical interest to determine the total amount of light that is scattered or absorbed by the sphere. This may be calculated by evaluating the Poynting vector and integrating it over all directions. With the help of the orthogonality relations that exist between the associated Legendre functions it is possible to express the integrals in terms of the coefficients ${}^{e}B_l$ and ${}^{m}B_l$. These calculations, which are somewhat lengthy, are carried out in full in the paper by Mie.†

The total energy lost from the incident wave, i.e. the sum of the scattered and the absorbed energy, may be determined in an alternative way, namely by the use of the optical cross-section theorem [§13.6 (25)] which expresses the extinction cross-section Q of an obstacle of arbitrary shape and the forward scattering amplitude by the formula

$$Q = \frac{4\pi}{k}\mathcal{I}\left\{\frac{\mathbf{e}\cdot\mathbf{a}(\mathbf{s}_0)}{\mathbf{e}^2}\right\}. \tag{98}$$

it being assumed that the scatterer is situated in free space.

Let us apply the general formula (98), with k replaced by $k^{(\mathrm{I})}$, to a spherical obstacle. According to (58) the amplitude component of the scattered wave in the direction of the electric vector of the incident wave ($\phi = 0$), for forward scattering ($\theta = 0$), is given by

$$(E_\theta^{(s)})_{\theta=\phi=0} = -\frac{1}{k^{(\mathrm{I})}}\frac{1}{r}\sum_{l=1}^{\infty}\left\{{}^{e}B_l\xi_l^{(1)\prime}(k^{(\mathrm{I})}r)[P_l^{(1)\prime}(\cos\theta)\sin\theta]_{\theta=0}\right.$$
$$\left.-\mathrm{i}\,{}^{m}B_l\xi_l^{(1)}(k^{(\mathrm{I})}r)\left[P_l^{(1)}(\cos\theta)\frac{1}{\sin\theta}\right]_{\theta=0}\right\}. \tag{99}$$

* The dispersion of polarization and polychroism was investigated by M. A. Schirmann *Ann. d. Physik*, (4), **59** (1919), 493.

† G. Mie, *loc. cit.*, pp. 432–436.

https://doi.org/10.1017/9781108769914.017 Published online by Cambridge University Press

The two terms involving the associated Legendre functions can easily be evaluated from the expansion*

$$P_l^{(m)}(x) = \frac{1}{2^m m!}\frac{(l+m)!}{(l-m)!}(1-x^2)^{m/2}\left[1 + c_1\left(\frac{1-x}{2}\right) + c_2\left(\frac{1-x}{2}\right)^2 + \cdots\right], \quad (100)$$

where c_1, c_2, ... depend on l and m only. From (100) and from the derivative of this expression we find that

$$\left(\frac{P_l^{(1)}(\cos\theta)}{\sin\theta}\right)_{\theta=0} = \tfrac{1}{2}l(l+1), \qquad [P_l^{(1)\prime}(\cos\theta)\sin\theta]_{\theta=0} = -\tfrac{1}{2}l(l+1). \quad (101)$$

On substituting from (101) in (99) and using the asymptotic approximation (74) and (76) for $\zeta_l^{(1)}$ and $\zeta_l^{(1)\prime}$, we obtain

$$(E_\theta^{(s)})_{\theta=\phi=0} = \frac{1}{2k^{(1)}}\frac{e^{ik^{(1)}r}}{r}\sum_{l=1}^{\infty}(-i)^l l(l+1)[{}^eB_l + {}^mB_l]. \quad (102)$$

Remembering that the incident field was taken to be of unit amplitude ($\mathbf{e}^2 = 1$), the required quantity $\mathbf{e}\cdot\mathbf{a}(\mathbf{s}_0)/\mathbf{e}^2$ is the multiplier of $e^{ik^{(1)}r}/r$ in this expression; on substituting it in (98) and using the identity $\mathcal{I}(z) \equiv \mathcal{R}(-iz)$, which holds for any complex number z, we finally obtain the following expressions for the *extinction cross-section of a sphere*, in terms of the coefficients ${}^eB_l$ and ${}^mB_l$ which are given by (62):

$$Q = \frac{\lambda^{(1)2}}{2\pi}\mathcal{R}\sum_{l=1}^{\infty}(-i)^{l+1}l(l+1)({}^eB_l + {}^mB_l), \quad (103)$$

where $\mathcal{R}$ denotes the real part.

(b) Computational results

We shall now summarize the main computational results relating to total scattering, total absorption, and the extinction of a sphere.

We saw in §14.5.2 that when the sphere is very much smaller than the wavelength (Rayleigh scattering), only the first electric partial wave needs to be taken into account. The amplitude of the scattered wave is then proportional to $1/\lambda^{(1)2}$, so that the total scattering is inversely proportional to the fourth power of the wavelength. If we take into account the higher terms, which depend on the radius and the material constants, the total scattering becomes a very complicated function of the wavelength and shows selective properties.† In the case of gold, for example, even a very small sphere gives a maximum near $\lambda = 5500$ Å (see Fig. 14.12).

* See W. Magnus and F. Oberhettinger, *Formulas and Theorems for the Functions of Mathematical Physics* (New York, Chelsea Publishing Company, 1954), p. 54. The formula given by these authors differs from (100) by a multiplication factor $(-1)^m$. This difference arises from their use of a slightly different definition of the associated Legendre polynomials (see footnote on p. 772).

† An interesting example of selective scattering was provided by the phenomena observed in September 1950, when over a large part of Europe the sun (and the moon also) appeared deep blue. Spectrographic measurements of the 'blue' and normal suns gave the extinction curve of the layer causing the phenomena, and it was concluded that the blue colour was due to selective scattering by smoke, probably consisting of oil droplets, remarkably uniform in size, which had been carried by winds in the upper atmosphere from forest fires burning in Alberta [see R. Wilson, *Mon. Not. Roy. Astr. Soc.*, **111** (1951), 478].

https://doi.org/10.1017/9781108769914.017 Published online by Cambridge University Press

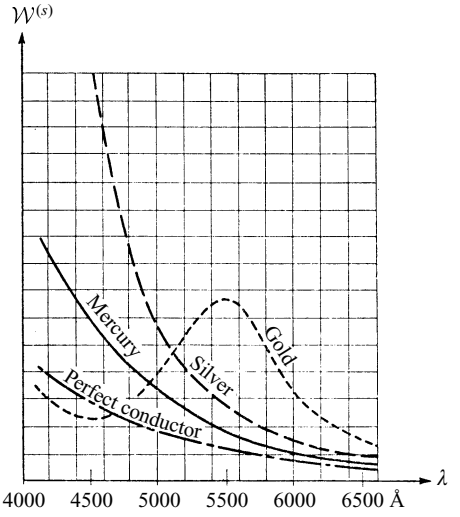

Fig. 14.12 Total scattering from very small particles ($a \to 0$) as a function of the wavelength. (After R. Feick, *Ann. d. Physik*, (4), **77** (1925), 582.)

Such maxima may be interpreted as a kind of resonance phenomena. Let us suppose that the sphere is not under the influence of the field of the incident beam of light, but that it performs a free electromagnetic oscillation. The frequency and the damping constant of this free vibration is obtained from the theory, by omitting in equations (56) those terms which do not contain the coefficients ${}^{e}B_l$ and ${}^{m}B_l$. The resulting equations are linear and homogeneous and have nontrivial solutions only if a consistency condition is satisfied. Each solution of the consistency equation corresponds to a damped proper vibration, and the frequency of these vibrations coincides very closely with the frequencies for which certain scattered partial waves have maxima of intensity.*

Calculations relating to scattering and extinction from spheres of finite radii, for selected values of the refractive index, have been carried out by many workers. The majority of the calculations concern dielectric spheres (n real) and spheres that are slightly absorbing. In Fig. 14.13 a typical curve, due to B. Goldberg, is shown for spheres of refractive index $n = 1.33$.† This is the refractive index of water, and the results are of interest in connection with the transmission of light by mist, clouds and fogs, in connection with the theory of the Wilson cloud chamber, etc. It is seen that the curve has a series of maxima and minima and that with increased radius the extinction

* Optical resonance was observed by R. W. Wood, *Phil. Mag.*, (6), **3** (1902), 396, from granular films and fogs of the alkali metals.

The proper vibrations of a sphere were studied by P. Debye, *Ann. d. Physik*, (4), **30** (1909), 73.

† This case was also investigated by H. Holl, *Optik*, **4** (1948), 173 and by H. G. Houghton and W. R. Chalker, *J. Opt. Soc. Amer.*, **39** (1949), 955. Similar curves relating to other values of the refractive index have been published by many writers, for example: M. D. Barnes and V. K. La Mer, *J. Col. Sci.*, **1** (1946), 79; M. D. Barnes, A. S. Kenyon, E. M. Zaiser and V. K. La Mer, *ibid.*, **2** (1947), 349; J. L. Greenstein (Harvard circ., 1937, No. 422); H. C. van de Hulst, *Rech. Astr. Observ. Utrecht*, **11**, Pt. 1 (1946), 43–51 and his book *Light Scattering by Small Particles* (New York, J. Wiley and Sons; London, Chapman and Hall, 1957), Chapter 13; R. Pendorf, *J. Opt. Soc. Amer.*, **46** (1956), 1001.

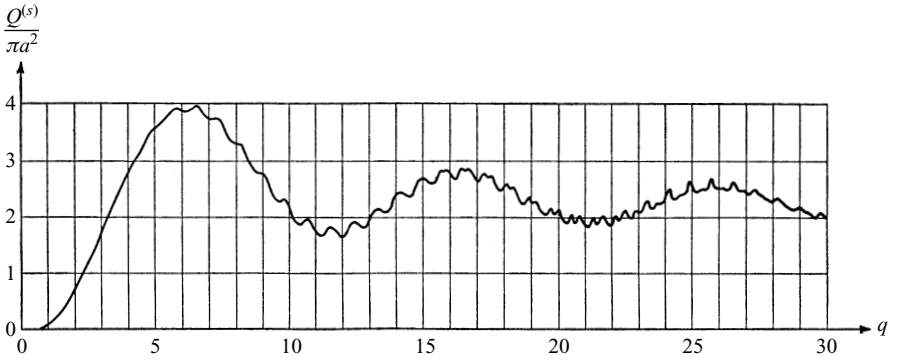

Fig. 14.13 The scattering cross-section of dielectric spheres of refractive index $n = 1.33$ as a function of the parameter $q = 2\pi a/\lambda$. (After B. Goldberg, *J. Opt. Soc.*, **43** (1953), 1221.)

cross-section tends to twice the geometrical cross-section, in agreement with §13.3 (25). The curve has also a fine structure, i.e. small subsidiary maxima and minima. Naturally, these small fluctuations are smoothed out if the scattering is caused by many spherical particles which are not of exactly the same size.

The extinction curves for dielectric spheres of other refractive indices exhibit similar behaviour. It may be shown that if n is not too different from unity all the curves have a first maximum for a value of q given by* $2q(n-1) \sim 4$, where Q may be as large as $4\pi a^2$.

For perfectly reflecting spheres† ($n \to \infty$) the first maximum of the extinction curve is found to be at $q = 1.2$, where $Q = 2.29\pi a^2$, and the first minimum at $q = 1.6$ where $Q = 2.12\pi a^2$. Thereafter there are slight oscillations and the curve approaches $2\pi a^2$ as $q \to \infty$.

The calculations relating to absorbing spheres are much more laborious and only a few special cases have been studied in detail. In Fig. 14.14 curves relating to scattering, absorption, and extinction by small spheres of iron are shown. For larger spheres, asymptotic formulae due to Jobst,‡ based on Mie's theory and on Debye's asymptotic expansions of the cylinder functions may be used for calculation. Weakly absorbing spheres have been studied by van de Hulst,§ and we show results of his calculations in Fig. 14.15. In this latter case the general behaviour of the extinction curves is seen to be similar to those of dielectric spheres, but even a very small conductivity is sufficient to smooth out the small undulations completely. As the conductivity is increased still further, the first minimum disappears altogether and the extinction curve rises asymptotically from the origin to 2; the absorption curves rise asymptotically from the origin to half this value.

Mie's theory may be tested experimentally by means of observations of light

* The quantity $2q(n-1)$ represents the phase shift suffered by a ray of light that traverses the sphere along a diameter. This is a useful parameter, and if n is not too different from unity the extinction curves plotted against it are very similar to each other.

† F. W. P. Götz, *Astr. Nachr.*, **255** (1935), 63 and J. L. Greenstein (*loc. cit.*).

‡ G. Jobst, *Ann. d. Physik*, (4), **76** (1925), 863.

§ H. C. van de Hulst, *Rech. Astr. Observ. Utrecht*, **11**, Part 2 (1949), 27.

https://doi.org/10.1017/9781108769914.017 Published online by Cambridge University Press

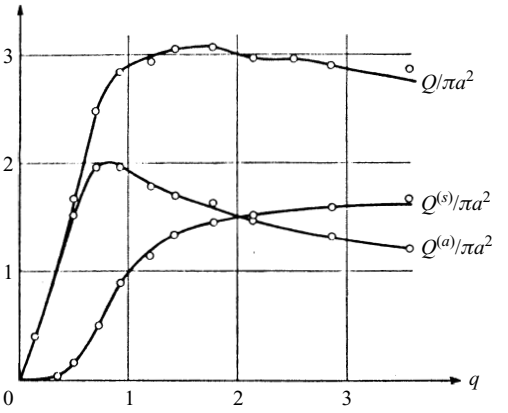

Fig. 14.14 The absorption cross-section $Q^{(a)}$, the scattering cross-section $Q^{(s)}$, and the extinction cross-section Q for iron spheres of various radii. $\hat{n} = 1.27 + 1.37\mathrm{i}$, $\lambda^{(1)} = 4200$ Å. [Based on computations of C. Schalén, *Uppsala Astr. Observ. Ann.*, **1**, No. 9 (1945).]

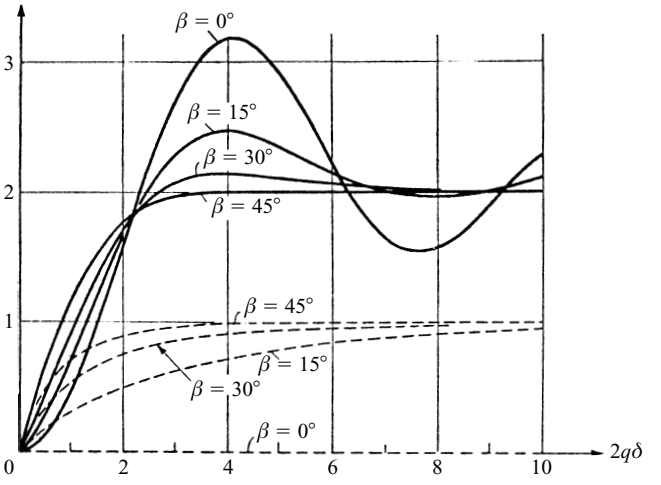

Fig. 14.15 The extinction curves $Q/\pi a^2$ (full lines) and the absorption curves $Q^{(a)}/\pi a^2$ (interrupted lines) for weakly absorbing spheres of refractive index $\hat{n} = (1 + \delta) + \mathrm{i}\delta \tan\beta$, where δ is real and small compared to unity. [After H. C. van de Hulst, *Rech. Astr. Obs. Utrecht*, **11**, Part 2 (1949), 28.]

scattered either by a single spherical particle, or by many particles (cloudy media, colloidal solutions). Such tests may be carried out with relative ease when the particles are large, but are rather troublesome when the diameter of each particle is of the order of a wavelength or smaller. La Mer and collaborators* succeeded in testing the theory from measurements of the angular distribution of scattered light as well as the total

* M. D. Barnes and V. K. La Mer, *J. Col. Sci.*, **1** (1946), 79; M. D. Barnes, A. S. Kenyon, E. M. Zaiser and V. K. La Mer, *ibid.*, **2** (1947), 349; I. Johnson and V. K. La Mer, *J. Amer. Chem. Soc.*, **69** (1947), 1184.

https://doi.org/10.1017/9781108769914.017 Published online by Cambridge University Press

scattering from sulphur sols in water, of particle diameter 3000 Å to 5000 Å. Light of vacuum wavelengths in the range from 2850 Å to 10,000 Å was used and a fair agreement with the predictions of Mie's theory was found. In some cases even the minute fluctuations (fine structure) of the extinction curve (see Fig. 14.13) were observed.

The scattering of light by particles of shapes other than spherical has been considered by some authors, but in general the analytical properties of the corresponding wave functions are much more complicated, so that rigorous solutions are of limited practical value.* Gans† and other workers discussed the scattering of electromagnetic waves by ellipsoids with dimensions small compared to the wavelength; a rigorous solution for an ellipsoid of arbitrary size has been published by Möglich.‡ The scattering from long circular conducting cylinders was studied as early as 1905 by Seitz§ and Ignatowsky‖ and the formulae obtained by them are similar to those of Mie relating to the sphere. Scattering by long circular dielectric cylinders and highly reflecting cylinders was investigated by Schaeffer and Grossmann.¶

* Approximate methods were developed by several authors. See, for example, R. W. Hart and E. W. Montroll, *J. Appl. Phys.*, **22** (1951), 376; E. W. Montroll and R. W. Hart, *ibid*., **22** (1951), 1278; E. W. Montroll and J. M. Greenberg, *Phys. Rev.*, **86** (1952), 889.

See also the review article by C. J. Bouwkamp, *Rep. Progr. Phys.* (London, Physical Society), **17** (1954), 35.

† R. Gans, *Ann. d. Physik*, (4), **37** (1912), 881; *ibid*. **47** (1915), 270.

‡ F. Möglich, *Ann. d. Physik*, (4), **83** (1927), 609.

§ W. Seitz, *Ann. d. Physik*, (4), **16** (1905), 746; *ibid*., **19** (1906), 554.

‖ W. v. Ignatowsky, *Ann. d. Physik*, (4), **18** (1905), 495.

¶ C. Schaeffer and F. Grossmann, *Ann. d. Physik*, (4), **31** (1910), 455; see also H. C. van de Hulst, *Astrophys. J.*, **112** (1950), 1.